“CFD ANALYSIS OF INCLINED JET IMPINGEMENT HEAT TRANSFER IN MICROCHANNEL”

Major project-II

submitted in partial fulfillment of the requirement for the award of the degree of

MASTER OF TECHNOLOGY

In

THERMAL ENGINEERING

By

ROHIT SAHU
2K15/THE/13

Under the guidance of

Mr. M. ZUNAID
ASSISTANT PROFESSOR

DEPARTMENT OF MECHANICAL ENGINEERING
DELHI TECHNOLOGICAL UNIVERSITY
NEW DELHI-110042
2015-17

Department of Mechanical Engineering

Delhi Technological University

Delhi

CERTIFICATE

This is to certify that the thesis entitled **"CFD Analysis of Inclined Jet Impingement Heat Transfer in Microchannel"** submitted by **Rohit Sahu (2K15/THE/13)**, during the session 2015-2017 for the award of M.Tech degree of Delhi Technological University, Delhi is absolutely based upon his work done under my supervision and guidance and that neither this thesis nor any part of it has been submitted for any degree/diploma or any other academic award.

The assistance and help received during the course of investigation have been fully acknowledged. He is a good student and I wish him good luck in future.

Date:

Mr. M. Zunaid

Assistant Professor

Department of Mechanical Engineering

Delhi Technological University

ACKNOWLEDGEMENT

To achieve success in any work, guidance plays an important role. It makes us put right amount of energy in the right direction and at right time to obtain the desired result. Express my sincere gratitude to my guide, **Mr. M. Zunaid,** Asst. Professor, Mechanical Engineering Department for giving valuable guidance during the course of this work, for his ever encouraging and timely moral support.

I am greatly thankful to **Dr. R. S. Mishra,** Professor and Head, Mechanical Engineering Department, Delhi Technological University, for his encouragement and inspiration for execution of the this work. I express my feelings of thanks to the entire faculty and staff, Department of Mechanical Engineering, Delhi Technological University, and Delhi for their help, inspiration and moral support, which went a long way in the successful completion of my report work.

ROHIT SAHU
2K15/THE/13
M.Tech (Thermal Engineering)
Delhi Technological University

DECLARATION

I, **Rohit Sahu**, hereby certify that the work which is being presented in this thesis entitled **"CFD Analysis of Inclined Jet Impingement Heat Transfer in Microchannel"**, is submitted, in the partial fulfillment of the requirements for degree of Master of Technology at Delhi Technological University is an authentic record of my own work carried under the supervision of **Mr. M. Zunaid**. I have not submitted the matter embodied in this seminar for the award of any other degree or diploma also it has not been directly copied from any source without giving its proper reference.

Date:

Place:

ROHIT SAHU
2K15/THE/13
M.Tech (Thermal Engineering)
Delhi Technological University

ABSTRACT

In this study inclined micro jet impingement heat sink used for electronic cooling application. Several particles and staggered inline micro-jet configuration will be used for study. In the present study fluid flow, there are two cases. In first case, pressure drop and heat transfer characteristics of rectangular micro- jet impingement heat sink have been analysed and validation is done by comparing experimental results with numerical results using computational fluid dynamics. In the second case the effectiveness of inclined jet impingement heat sink will be analyzed at various no. of jets for the maximum temperature-drop of fluid-solid interface. The shape optimization of a micro-jet heat sink with a grooved structure has been performed using a multi objective evolutionary algorithm in ANSYS CFX solver.

In the present study inclined micro jet impingement focus on electronic cooling in micro level. This study of heat sink focus on 3D micro channel for fluid flow analysis. The jets used have been placed at an inclination of 45^0 from the top surface of the impingement heat sink. during this process copper has been used as the solid material and water has been used as a cooling fluid. The optimum results were obtained by using the 13 micro-jets heat sink at an inclination of 45^0.

The study simulated in different micro-jets heat sink with 4, 5, 9, 13 and 16 no. of impingement jets at water as a fluid. During study simulation carried out on these no. of jets with 3 different diameters ie 0.1mm, 0.15mm & 0.2mm. After the simulation 13 jet impingement micro-jets heat sink shows maximum temperature drop between fluid & solid interface. During the simulation difference in temperature and heat transfer coefficient define maximum heat transfer through the impingement heat sink. The geometry of the micro-jet impingement heat sink is constructed in solid work design software and the simulation is done on ANSYS CFX.

CONTENTS

LIST OF TABLES

LIST OF FIGURES

ABBREVIATIONS

Symbol	Description
A	Base area of plate, m^2
A_{CS}	Cross-section area of nozzle, m^2
C_p	Specific Heat at Constant Pressure, J/kg-K
d_n	Nozzle diameter, m
ρ	Density of fluid, kg/ m^3
V	Volume of heat sink,m^3
m	Mass flow rate, kg/s
H_c	Height of the fluid Channel, m
h	Heat transfer coefficient, W/m^2 K
k	Thermal conductivity, W/mk
L	Length of the heat sink, mm
B	Width of the heat sink, mm
H	Height of the heat sink, mm
l_n	Vertical height of the micro-jet nozzle, mm
t_s	Thickness of the solid substrate base, mm
S_n	Interjet spacing, mm
n	Number of jets
q	Heat flux, W/cm^2
R_{th}	Thermal resistance, K/W
T_s	Temperature of solid, K
T_f	Temperature of the fluid, K

v	Velocity of fluid, m/sec
T_{b1}	Mean bulk temperature of fluid at inlet, K
T_{b2}	Mean bulk Temperature of fluid at outlet, K
ΔT_{max}	Maximum Temperature rise, K
T_{avg}	Average surface Temperature of fluid-solid interface, K
T_{max}	Maximum temperature of fluid-solid interface,K
R_e	Reynolds number
x,y,z	Cartesian coordinates

CHAPTER 1

INTRODUCTION

1.1 Micro channel

Micro-channels, have become very advanced in applications where very high heat transfer rates are happened. The development of microchannel trending as electronics equipment becomes more advanced and smaller in size with ongoing contiuous innovations. It offends thermal engineering challenges from a very high level of heat generation and the reduction of available surface area for heat dissipation. In the absence of sufficient heat dissipation, the running temperature of this components may exceed an undesired temperature level which is then increases the critical failure rate of the equipment. Therefore, this advanced electronic equipment with very high heat generation requires an efficient and compact device so as to provide proper cooling effect. In order to meet the cooling requirement, one need is to increase the heat transfer rate and therefore heat transfer coefficient (h) for a device. Since heat transfer coefficient is related to the nozzle diameter and mass flow rate. One promising solution to the problem is liquid cooling incorporating on channels.

1.2 Use of micro channel

Tuckerman and Pease was studied the fluid flow for heat transfer as a scope of Ph.D. study. The publication title on “High Performance Heat Sinking in VLSI” was first study on micro channel for heat transfer. Their good work on the micro level have innovative research to focus on the field as micro channel and fluid flow in the channel has recognized such a high performance fluid heat transfer through the micro channel.

As the study of micro channel in different category which assist the “microchannel” as heat transfer body from the substrates fluid. The scope of micro channels the debate in this topic between researchers in the field. the following used as study research factor in different “*D*”, being the smallest.

The micro channel describes the flow field in different category which can be operated the substrate fluid dynamics. As the channel describe in flow field in category of micro channel.

- Micro channels:-1μm < D <100μm
- Mini channel:- 100μm < D < 1 mm
- Compact Passage:- 1 mm < D < 6 mm
- Conventional Passage:- 6 mm < D

1.3 Jet impingement

Micro-channel and jet impingement give use full means for convective heat transfer coefficient due to large transfer of heat and mass transfer rate. Micro channel is mostly used in industrial applications like as tempering of material, annealing, plastic cooling and paper fabric dry process. Due to the geometrical condition heat transfer of multiple jet substantially from single jets. The spacing between the jets is greater effect on the amount of heat transfer. The complexity as comparing result, a multiple jets geometry dilution a large no. of militating factors. For the comparing the result another development correlation as in Sung and Mudawar [22]. Reynolds number (Re), nozzle to impingement surface dimension, H/D and angle of impingement are parameter to determine jet configuration. Sung & Mudawar [22] and others have carried out various experimental and numerical simulation on microchannel and jet-impingement system reduce the value of pressure drop & temperature gradient in microchannel as application on device of electronic, jet impingement in micro channel in jet condition zone thermal boundary layer development during fluid flow.

1.4 Coolants used in micro-channel heat sink

Numerous coolants are available in the market that can be employed in the heat sink for the removal of heat energy. A commonly used coolant in a heat sink is water, because of its better thermal properties. However, for better cooling performance of the micro-channel cooler nano-fluids can be used. But in the recent trend , it has been seen that cooling performances of performance fluids like PF5052, PF5060 etc are quite superior than their counterparts.

1.5 Materials used for the heat sink

Generally the thermal property which a heat sink material should possess is high thermal conductivity for better heat dissipation. A lot of materials are available in the market such as silicon, copper, aluminium etc that can be used for heat sink.

Table 1: Thermal properties of some metals used as a sink material

Material	Thermal Conductivity (k)	Thermal Expansion coefficient (α)
Aluminium	237 (W/m-K)	23.1 (μm/m-K)
Silicon	149 (W/m-K)	2.60 (μm/m-K)
Copper	401 (W/m-K)	17.1 (μm/m-K)

1.6 Computational fluid dynamics (CFD)

The branch of a multiple objective fluid dynamics problem that provides a cost effective means of simulating the real flows by a numerical solutions of the governing equations is known as Computational Fluid Dynamics (CFD.).The Navier–Stokes equations, one of the governing equations for Newtonian fluid dynamics have been known for over 100 years. Still today the development of reduced form of these equations a major and active field of research, particularly the turbulent closure problem of Reynolds averaged Navier-Stokes equations. But in case of non-Newtonian fluid dynamics, two phase flows and chemically reacting flows, theoretical development is at a lesser advanced stage.

In this method i.e. Computational technique, the governing partial differential equations replaced by a system of algebraic equations that can be solved very easily by the help of computers. One of the major reasons for the rise and emergence of CFD is the steady enhancement in computer power since 1960s.It allowed testing of situations which are very tough or impossible to be measured experimentally and are not amenable to analytic solution.

Experimental methods play a major role in analyzing and validating the limits of different approximations to the governing equations, mainly rig tests and wind tunnel thus providing a cost effective alternative to full scale testing. The analytic solutions

cannot be achieved for most practical applications due to the extreme complexity of flow governing equations.

In the computational fluid dynamic problem we used different code in authorized ansys. In this condition the CFD conclude problem to problem as per data given. The method constraint in the alternative testing scale. In using the thermal design problem CFD provided the simulation on the various flow technique as per the problem.

CFD base on different problem on different situation on grid data it noted that fluid flow condition in micro channel. It is noted the segment of analytic solution describe the condition of fluid flow condition.

1.7 Application of CFD

1.7.1 **Aerospace:** - Various methods of CFD are used in many aerospace applications for the role of predicting component performance and also as an integral part of the design cycle. The applications are many like flow around an aircraft etc.

1.7.2 **Automotive: -** In the field of automotive applications CFD is used for modeling the cars aerodynamics to reduce drag and optimize the down force under different operating conditions and also in other fields like auxiliary systems, engine components etc.

1.7.3 **Biomedical: -** CFD is used to design and simulate the blood flow in the heart vessels, inhalers, flow in heart assist devices and other equipment like drug and anesthetic devices from university of buffalo.

1.7.4 **Chemical Engineering: -** Applications of CFD in the field of chemical engineering are vast and surplus such as petrochemicals, pollution control, fertilizers, food processing, waste treatment recycle etc.

1.7.5 **Power Generation: -**In the field of power sector CFD finds applications in the analysis of economizer, super heaters, pulverized coal combustion, low NOx burner design and in other areas to improve performance and efficiency of the plant.

1.7.6 **Electronic systems: -** The demand for quieter, smaller, more powerful, safer and reliable electronic equipment and various thermal challenges faced by manufactures highlights the increasing demand for easy to use, accurate and cheap computational design tools to overcome complex thermal problems related to their cooling. It is the thermal analysis of electronic system by thermal management solution(TMC).

1.8 Steps of CFD

- Divide the fluid volume (surface) up into manageable chunks (gridding)
- Equation to be simplify at required condition
- boundary condition must be set
- Initialization of grid values
- Simplify the equation through the step grid at the required set point.

1.9 Advantages

In CFD process there are following advantage carried out. It dominate the various step process but it quiet effective to generation 3d volume. The generation process take less time as time take manually operated process.

- In CFD process carried out great time reduction and reduction in cost.
- There is a possibility analyze different problem which are very difficult and dangerous.
- CFD technique offer analyze the problem in capacity of limit in over its limit.
- Practical unlimited in level of detail.
- For analyze the result plot various graph for validation the result in deferent purpose use.
- For the good result simplification has been quite simple in mode of process.
- Several incomplete modal to describe the turbulence, multiphase and other difficulties problem.
- Untrained user has tendency pc output true always.

1.10 Disadvantages

- Easy to excess and law investment lead to over trading.
- Initially cost provided through the set up more as par data.

1.11 CFD code

CFD code use in different category in various applications. The use of these code we can apply in the generation tool which an associate in cfd analysis.

- **CFD commercial code**: STAR CD, FLUIENT, CFX, CFDESIGN, FLUIDYN etc.
- **CFD research code:** COOLFLUID, CFDSHIP IOWA etc.
- **CFD public code:** WINPIPED, HYDRO etc**.**
- Other CFD code use in generation software such as GEMBIT and grid visualization such as ADINA- AUI CFX-Post, COMSO, ENSIGHT, FIELDVIEW, Hyper View ETC.

1.12 CFD Process

- The purpose of CFD use with respect to the code applies in various applications such as separated the bubbly flow through domain.
- In the application we seen the massive flow, uniform flow and unsteady flow. In the proses which provide the conjugate configuration rate in the code assign.
- With respect to the code we can apply various other application such that multiphase fluid. Marine, biomedical etc.
- The flow tendency in various manner judges by the code applies on it. It is configure the step in apply the code.
- It leads to apply the code as per the step required in generation process. During the process configuration said the next step to lead. If there drawback than post process to apply.

  STEPS:

  - Layout the geometry
  - Apply the physics
  - Generate mesh
  - Solution
  - Report
  - Feedback

1.13 Background Information

The science and practice of achieving approximate numerical solution using digital computers is known as Computational Mechanics. When this approach is applied in the field of problems concerned with thermal and fluid problems, it is generally termed as Computational Fluid Dynamics (CFD). Thus CFD is primarily a branch of continuum mechanics that deals with numerical simulation of heat transfer and fluid flow problems.

The basic fundamental of almost all CFD problems are Naiver–Stokes equations, which defined many single-phase (gas or liquid, but not both) fluid flows. The Euler equations are achieved by simplifying these equations by removing terms defining viscous action. The full potential equations can be obtained by doing further simplification by eliminating terms describing vorticity. For small perturbations in subsonic and supersonic flows equations could be linearized to yield the linearized potential equations.

Historically, a method was first developed to solve the linearization potential equations. Two dimensional (2D) methods were developed using flow over a cylinder by taking air foil as reference selection. Even though they failed, these calculations set the basis for modern CFD. The computer power available paced development of three-dimensional methods. Los Alamos National Lab can be considered as the place where the first work using computers to model fluid flow governed by the Navier-Stokes equation. Francis H. Harlow, who is considered as one of the pioneers of CFD led this group and they developed various types of numerical methods like Particle-in-cell method, Fluid-incell method, Vorticity stream function method, Marker-and-cell method in order simulate transient two-dimensional fluid flows. The initially treatment of strongly contorting incompressible flows in the world were method of the vorticity-stream-function for 2D, transient, incompressible flow by Fromm's. Today different codes are used in the development of many submarines, helicopters, surface ship and more recently wind turbines. Many codes have also been used for modelling such things as high speed trains, racing yachts and also in jet impingement and micro-channel cooling technology. Now days in to achieve greater high heat flux removal and thereby reducing the high temperature and pressure gradient along channel flow, a new field of research is trying to harness the two cooling technologies (microchannel and jet impingement cooling).

1.14 Objectives

- The characteristics of fluid flow are investigated by modelling single-phase fluid flow and heat transfer in a micro-channel jet impingement with the help of CFD. Numerical model has been used to analyse the three dimensional micro-channel jet impingement fluid flows by assuming the flow to be fully developed flow.
- To examine the temperature variation characteristics of 4 jet inclind impingement heat sink by comparing with 4 jet straight impingement heat sink model at different heat flux values.
- To examine the pressure variation and temperature variation characteristics at solid-fluid interface of heat sink for different jet configurations and different jet diameters. Optimize the result with best configuration of inclined jet model which have better utilization of cooling fluid and have a good temperature drop characteristic

CHAPTER 2

LITERATURE REVIEW

2.1 Experimental and numerical studies on micro-channel heat sink:

Thermal control has become a critical factor in the design of electronic equipment because of the recent trends in the electronic industries towards increased miniaturization of components and device heat dissipation. A great demand on the system performance and reliability also intensifies the needs for a better thermal management. L.T. Yeh[3] represented a review of heat transfer technologies in electronic equipment.

In the history of micro-channel design various research has to be performed on experimental comparison of micro-channel heat exchanger with micro-channel porous media. The effect of the dimension on heat transfer was analyzed numerically. It was emphasized that the heat transfer performance of the micro-channel heat exchanger using porous media is better than using of micro-channels, but the pressure drop of the former is much larger.

Knight et al.[2] represented the heat sink optimization with application to microchannels. The equations governing the fluid dynamics and combined conduction/convection heat transfer in a heat sink are presented in a dimensionless form for both laminar and turbulent flow. This scheme presented for solving these equations permit the determination of heat sink dimensions that display the lowest thermal resistance between the hottest portion of the heat sink.

Webb et al.[4] et al.have done experimental work to explore the micro-channel cooling benefits of water-based cooling-fluids containing small concentrations of Al_2O_3. It was observed that the presence of Al_2O_3 enhances the single-phase heat transfer coefficient in a jet impingement model, especially for laminar flow.For two-phase cooling, this additive caused catastrophic failure by depositing into large clusters near the channel exit due to localized evaporation once boiling commenced.

Peng et al. [6] investigated experimentally the single-phase forced convective heat transfer micro-channel structures with small rectangular channels having hydraulic diameters of 0.133–0.367 mm for different types of geometric configurations. The results shows heat

transfer and flow characteristics. The laminar heat transfer found to be dependent upon the aspect ratio i.e. the ratio of hydraulic diameter to the centre to centre distance of micro-channels.

Mala et al.[7] observed that the prediction of heat transfer in micro-channels becomes difficult with increase in complicacy of the geometry of the micro-channels, requiring three dimensional analysis of heat transfer in both solid and liquid phases. Computational Fluid Dynamics (CFD) models were implemented in order to study and optimize the thermal and hydraulic performance of micro channel heat sinks. Despite the small width of the channels, the conventional Navier Stokes and energy conservation equations still apply to the flow due to the continuum of the working fluid where the channel width is many times larger than the mean free path of liquid molecules (water). The micro-channel is characterized by the laminar flow in it, due to the small hydraulic diameter of the channel which results in low Reynolds numbers.

Fedorov et al. [10] developed a three dimensional model to investigate the conjugate heat transfer in a micro channel heat sink with the same channel geometry used in the experimental work done. This investigation indicated that the average channel wall temperature along the flow direction was nearly uniform except in the region close to the channel inlet, where very large temperature gradients were observed. This allowed them to conclude that the thermo–properties are temperature dependent.

Ambatipudi et al.[11] developed a reliable experimental device and adequate methodology to characterize the flow and convective heat transfer in flat micro channels. The study was concerned with measurement of pressure drop and heat transfer by a Newtonian fluid flow inside a flat micro channel of rectangular cross-section whose aspect ratio is sufficiently high that the flow can be considered two dimensional They considered the hydraulic diameter as twice of the channel height. The mathematical model used to describe the convective heat transfer between the walls and the fluid takes into account the whole field (solidwall and fluid layer) and the coupling between the conduction and the convection modes. Finally they concluded that the conventional laws and correlations describing the flow and convective heat transfer in ducts of large dimension are directly applicable to the microchannels of heights between 500 and 50 microns.

Qu et al. [12-13] have performed experimental and numerical investigations of pressure drop and heat transfer characteristics of single-phase laminar flow in 0.231 mm by 0.713 mm channels. Deionized water was employed as the cooling liquid and two heat flux levels,100W/cm^2 and 200 W/cm^2.Good agreement was found between the measurements and numerical predictions, validating the use of conventional Navier–Stokes equations for micro channels. For the channel bottom wall, much higher heat flux and Nusselt number values are encountered near the channel inlet.

Toh et al.[14] has reviewed the experimental and numerical computation results on fluid flow distribution, heat transfer and combination thereof, available in the open literature. They have found that the experiments with single channels are in good agreement with predictions using the published correlations. The review consists of two parts. In the first, the main methods to control flow distribution were reviewed. Several different designs of inlet/outlet chambers were presented together with corresponding models used for optimization of flow distribution.

Garimella et al.[15] theoretically analyzed the thermal performance of parallel flow micro heat exchanger subjected to constant external heat transfer.The model equations predicts temperature distributions as well as effectiveness of the heatexchanger.Moreover,the model can be used when the individual fluids are subjected to either equal or unequal amounts of external heat transfer.

Liu et al.[16-17] have studied numerically on fluid flow and heat transfer in micro channels and confirmed that the behaviour of micro channels is quite similar to that of conventional channels. And their analysis showed that conventional correlations offer reliable predictions for the laminar flow characteristics in rectangular micro channels over a hydraulic diameter in the range of 244–974 μm.They have further verified the capacity of conventional theory to predict the hydrodynamic and thermal features of laminar Newtonian in compressible flows in micro channels in the range of hydraulic diameter from D_h =15 μm to D_h = 401μm .They have compared their results with the data available in open literature. The theoretical models were subdivided in two groups depending on the degree of correctness of the assumptions. The first group includes the simplest one-dimensional models assuming uniform heat flux, constant heat transfer coefficient, etc. The comparison of these models with experiment shows significant discrepancy between the measurements and the theoretical predictions.

Foli K et al.[19] represented the optimization of micro heat exchangers with the help of CFD, an analytical approach and multi objective evolutionary algorithms. Their studies have established that the thermal performance of a microchhanel depends on its grometric parameters and flow conditions. Defines two approaches for determining the optimal geometric parameters of the microchannels in micro heatexchangers. One approach combines CFD analysis with an analytical method of calculating the optimal geometric parameters of micro heatexchangers. The second approach involves the usage of multi objective genetic algorithms in combination with CFD.

2.2 Experimental and numerical studies on jet impingement heat sink:

The recent challenges caused by the decreasing size of ultra-large scale integrated (ULSI) circuits of power electronics to dissipate the high heat-flux have encouraged researchers to develop new cooling techniques at the microlevel.With the air cooling techniques reaching their limits, the liquid cooling through a micro-channel heat sink has provided efficient solutions for the high heat-flux management of electronics.

Tuckerman et al.[1] were the first to examine liquid flow micro-channel heat sinks. They accomplished experimentation on three micro-channels with widths of 50, 55 and 56 μm, and depths of 287, 302 and 320 μm, and developed a new concept of micro-cooling for researchers. One of the heat sinks could remove a heat flux as high as 790 W/cm^2 . The liquid flows from one end to the other through the narrow parallel channels leave higher temperatures at the inlet-side and lower temperatures at the outlet-side [18-19]. The temperature non-uniformity on the heated surface (consequently chip surface) induces thermal gradients, which reduces the life of the electronics. Jet impingement cooling offers new avenues for high heat-flux management of an entire surface as well as hot spots in power electronics with relatively more uniform temperature distribution over the chip surface. Recently, the applications of micro-jet impingements on the substrate were proposed to achieve higher temperature uniformity and hot spot management of electronics.

Garimella et al.[5] characterized a single submerged and confined jet for local heat transfer. They examined the effects of dn, Hc/dn, ln/dn, and flow rate on heat transfer and proposed correlations based on the jet Reynolds number. He concluded that the H_c/d_n ratio had a negligible effect on the heat transfer, and any improvement in heat transfer was due to an increase in velocity. They proposed the correlations for heat transfer.

Wu et al.[8] examined experimentally the heat transfer characteristics of 500 and 550 μm single jet as well as a jet array with Hc ranging from 200 to 3,000 μm. They obtained an area-averaged heat transfer coefficient of 320 W/m^2 K for a 500 μm single jet with H_c = 750 μm at a pressure drop of about 34,474 Pa. They also reported a higher cooling efficiency at lower driving pressures, which decreased with further increases in driving pressure.

Lee et al.[9] carried out comparative analysis of the micro-channels and jet impingement cooling.They concluded that micro-channel cooling is preferable for a heated surface smaller than 70 mm × 70 mm, and jet impingement is comparable to or better than micro-channel cooling for a large target plate with a proper arrangement of spent flow after impingements. With the advent of MEMS technology and advanced fabrication processes, the production of micro-scale jets has become more convenient than before. The potential of micro-jet impingement cooling of electronics has motivated researchers to examine liquid micro-jet impingements heat sinks analytically, numerically and experimentally.

Fabbri et al.[18] examined impinging jet arrays in a circular pattern with three different radial and circumferential pitches of 1, 2 and 3 mm. They investigated free jets of both water and FC-40 at Reynolds numbers ranging from 73 to 3,813, and reported heat transfer coefficients ranging from 6,000 to 60,000 W/m^2K.

Sung et al.[20] proposed a hybrid cooling scheme for electronics cooling, which combines the cooling benefits of micro-channel and jet impingement. They carried out experimental and numerical analysis of slot jets impingements in the micro-channels that showed low temperature and small temperature gradients across the surface.

Luo et al.[21] performed numerical and experimental analysis of a microjet based cooling system for the thermal management of high power light emitting diodes (LEDs). In their study, a 2 × 2 LED chip array of size 1 mm × 1 mm was embedded in a 15 mm × 15 mm substrate. Their system showed a maximum rise in chip temperature of 36.7 ^{0}C with an input power of 5.6 W and flow rate of 9.7 ml/s.

In a recent study, Husain et al.[22] reported on numerical analysis and optimization of a micro-jet impingement heat sink for high power LED cooling. Macro-jet impingement cooling has been the subject of intense research with their applications to macro-heat sinks and turbomachines before micro-jet impingement was applied to electronics cooling and micro-systems. Jet impingement has a rich history with most of the investigations based on air jet impingements.

Michna et al.[24] investigated a single confined submerged micro-jet that impinged on a square heated surface.They achieved heat fluxes of up to 4 × 106 W/m^2 with a temperature rise of approximately 50^{0}C. Their study revealed a higher pressure-loss coefficient than the available correlations for orifice tubes under $Re_d \leq 500$. In a later study, they

experimentally investigated an array of micro-jets for stagnation heat transfer and obtained a maximum of 11 × 106 W/m^2 heat flux for fluid inlet to surface temperature difference of less than 30 ^{0}C. They observed that Reynolds number, Prandtl number, and area ratio (total area of jets divided by the surface area) have significant effects on heat transfer.

Paz et al. [26] carried out numerical investigation of multi-micro-jet impingement cooling analysis of turbine blade. They observed that increasing the H/D ratio from 1.58 to 3 the overall heat transfer coefficient was decreased.

Heo et al.[27] investigated inclined elliptic jet for cross-flow analysis through numerical methods. They observed that the size of the recirculation region just upstream of the jet and length of the potential core of the jet significantly affect the heat transfer process. Recently, optimization methods with numerical analyses have been applied to several micro-scale transport systems to enhance the efficiency and decrease the power input.

Husain et al.[25,28-29] and Samad et al.[23] proposed optimization models for conventional and micro-scale thermofluid systems. Although there is a great deal of literature existed on macro-scale air jet impingement cooling, there is a paucity of reports on micro-scale multiple liquid-jet impingements and their optimization for heat-flux management of electronics and other micro-scale applications, where the flow is mostly laminar and the allowed flow-rate and pressure-drop are relatively small.

2.3 Summarizing remarks

As these case studies illustrate,there are many different numerical solutions to the Navier-Stokes equations that have been implemented successfully on the simple microchannels as well as in jet impingement models with different thermophysical and designing parameters like Reynold no., jet diameter, mass flow rate, No. of jets and type of cooling fluid. But the recent challenges caused by the decreasing size of ultra-large scale integrated circuits of power electronics need always improvement in better heat dissipation. Hence the current thesis work is directed toward addressing an improvement in heat transfer by performing a thermal and fluid flow analysis in an inclined jet impingement model with different jet configurations.

CHAPTER 3

METHODOLOGY/ MODEL DESCRIPTION

3.1 Numerical formulation and boundry conditions

In the analysis which was performed on the fluid flow domain and heat transfer through the model, in order to provide a cooling effect on the micro-jet impingement heat sink water is taken as cooling fluid where mass flow rate and heat flux is being kept constant. The equations used during the process include governing equation through the channel as fluid flow, conservation of mass, momentum and energy equation in flow field.

MASS CONSERVATION EQUATION

$$\frac{\partial(\rho u)}{\partial x} = 0 \qquad ..(1)$$

MOMENTUM CONSERVATION EQUATION

$$\frac{\partial(\rho uv)}{\partial x} = -\frac{\partial \rho}{\partial x} + \frac{\partial\left(\mu\frac{\partial u}{\partial x}\right)}{\partial x} \qquad ..(2)$$

ENERGY CONSERVATION EQUATION

$$\frac{\partial(\rho C_p\, u\, T)}{\partial x} = \frac{\partial(k\frac{\partial T}{\partial x})}{\partial x} \qquad ..(3)$$

Simulation provides the flow field in ansys. It was accomplish during various fluid flow through in it. The simulation define simple hexahedral mesh generated specified computational fluid domain. During iteration solid and fluid domain are classified in a conjugated manner.

It recommended hexahedral mesh in particular computational domain during fluid flow. For study heat sink optimized specified parameter in a channel fluid wall in fluid domain except solid fluid domain interface at bottom of channel kept adiabatic.

In a channel uniform heat flux provided from the solid substrate base towards the cooling fluid and no slip condition(v=0) is assumed at solid-fluid interface. During the

flow in internal wall of nozzle throughout it kept inclined from the top surface of the channel.

HEAT FLUX EQUATION:

$$\frac{Q}{A} = h * (T_2 - T_1)$$

$$q = h * (T_2 - T_1) \quad ..(4)$$

NUSSELT NO:

$$Nu = \frac{hD_C}{k}$$

HEAT TRANSFER COEFFICIENT:

$$h = \frac{q}{(T_2 - T_1)} \quad ..(5)$$

CHARACTERISTICS DIAMETRE:

$$D_C = \frac{4A}{P} \quad ..(6)$$

A=H*B

P=2(H+B)

ENERGY CONTAINED BY THE FLUID:

$$Q = M\ Cp\ (T_2 - T_1) \quad ..(7)$$

M=ρV

3.2 Assumptions and Boundary conditions

1. No slip condition between solid and fluid interface domain and assuming adiabatic condition except bottom surface.
2. Uniform inlet temperature and static pressure were given at the entry of the channel.
3. Temperature assumed to be constant in interface fluid and solid domain.
4. Outlet of the channel is based on mass flow rate.

Description of problem

A copper-based various micro-jets impingement heat sink model, as shown in below figures was designed on the upper-side of a heat sink with multiple micro-jet nozzles. The micro-jet nozzles were designed on the solid substrate and a fluid domain was created to allow fluid to pass through this jets. The fluid micro-jets strike at the heated solid surface and the flow turns to the radial direction at the same time removing heat from the bottom surface and reaches to the outlet port of the heat sink, as shown in Fig. For conservative analysis in the CFD, the constraint dimensions of the jet impingement heat sink model design shown in Fig. 1 were 12mm×12 mm×0.8mm. The total thickness of the impingement heat sink plate was 800 μm, in which multiple micro-jets were designed. Since due the symmetrycity of the heat sink one half of the heat sink was taken in the computational analysis about the central plane. The thickness of the solid substrate base was 100 μm, and the depth of the fluid domain was 300 μm. The different parameters that affect the performance of the impingement heat sink are:

- Thickness of the solid substrate base (t_s).
- Micro-jet nozzle diameter (d_n).
- Vertical height of the micro-jet nozzle (l_n).
- Interjet spacing (S_n).
- Height of the fluid domain (H_c).

The distribution of the micro-jets, i.e. the inclined 4 jet, 5 jet, 9 jet, 13-jet and 16 jet arrays shown in Figure 3.1, 3.3, 3.5, 3.7 and 3.9. The geometric parameters, l_n and t_s, were kept constant throughout the analysis.

3.3 Geometry of the micro-jet impingement heat sink

For this computational fluid dynamics problem, the geometry of the heat sink was constructed using solid works, and was imported to ANSYS workbench CFX for further meshing and CFD simulations.

For creating geometry, first the heat sink was made in solid works as per the dimensions given in tables and was named as solid part while fluid channel was created of the same

dimensions as of the rectangular slot along the length of heat sink for proper mating and was given the name of fluid part.

Both parts were created separately using solid works and were later assembled by inserting fluid channel in solid heat sink using the insert components and mate option in solid works.

Problem 1: Inclined 4 jet model

Table 3.1: Dimensions of the 4 micro-jet heat sink

A_{cs} (mm)	H_c (mm)	t_s (mm)	d_n (mm)	l_n (mm)	S_n (mm)
12×12	0.3	0.1	0.1	0.5	6

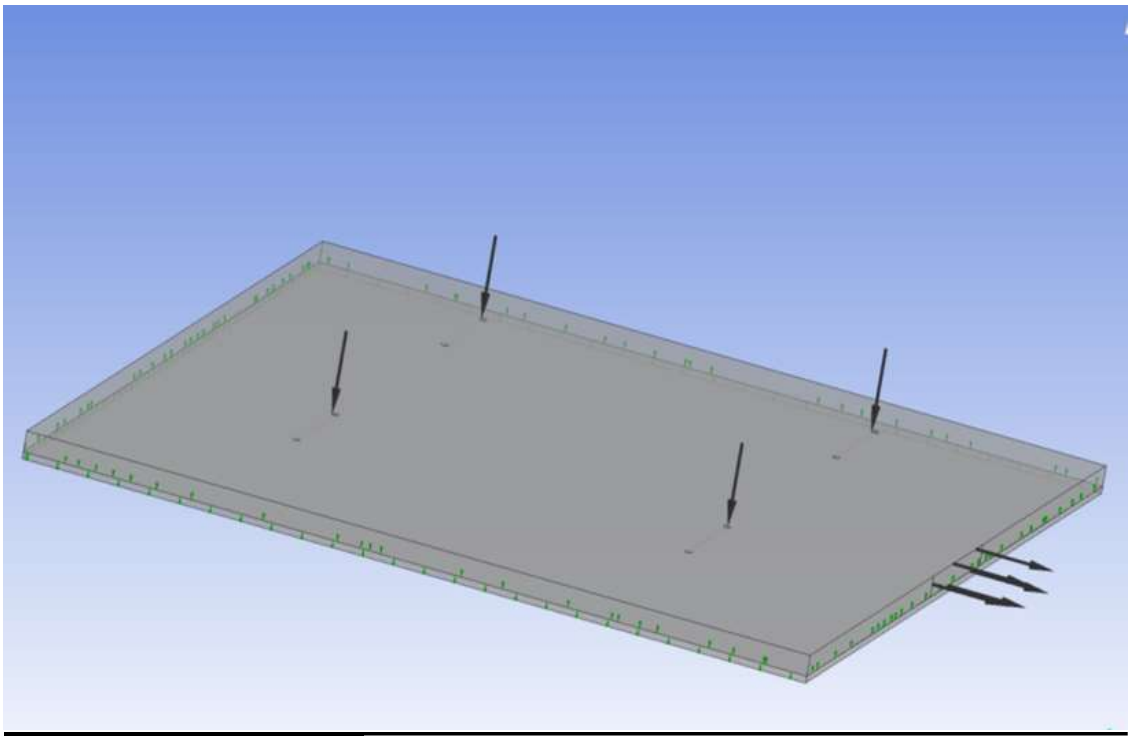

Figure 3.1: Geometry of the 4 micro-jet impingement heat sink.

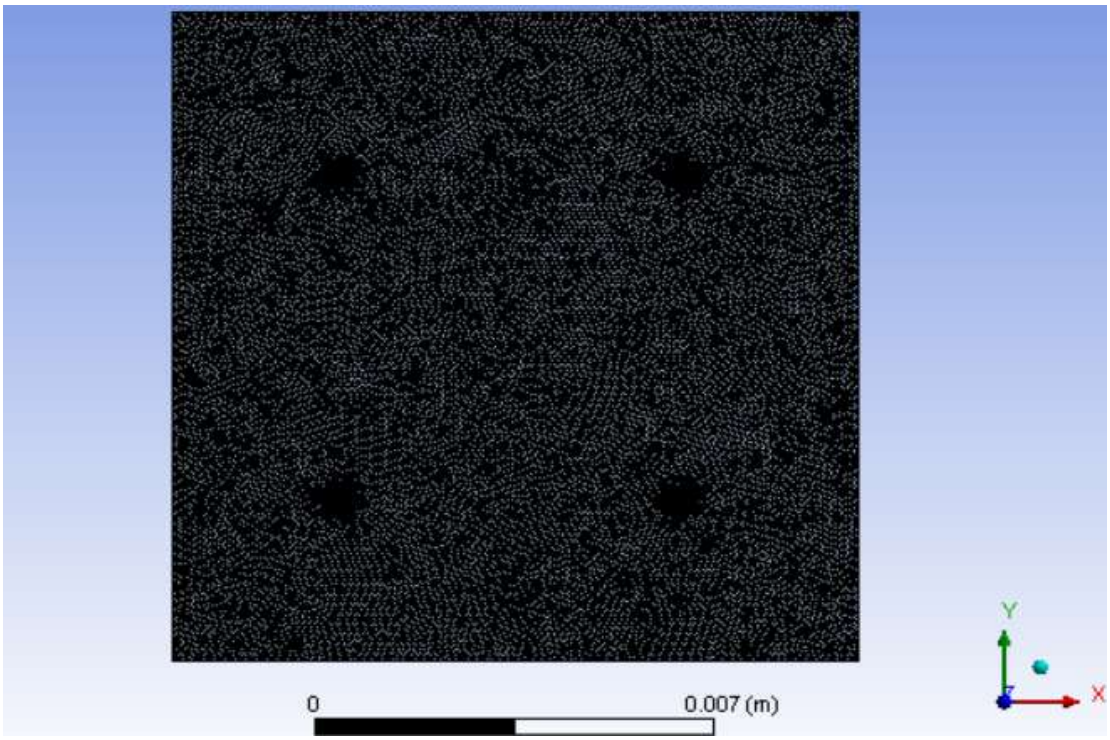

Figure 3.2: Meshing of the 4 micro-jet impingement heat sink in ANSYS CFX.

Mesh details -

Physics preference	CFD
Solver preference	CFX
Use Advanced Size Function	On: Proximity and Curvature
Relevance Center	Coarse
Smoothing	Medium
Transition	Slow
Transition ratio	0.77
Minimum size	Default (8.4707e-006 m)
Maximum face size	Default (8.4707e-004 m)
Maximum size	Default (1.6941e-003 m)
Nodes	1104008
Elements	3382134

The mesh was generated using proximity on option. For the micro-jet impingement heat sink the mesh was created as a structured mesh and for checking the solutions the mesh was made finer and the solutions obtained were mesh independent. After the meshing, the named selection were given, which are to be considered as boundary conditions.

Problem 2: Inclined 5 jet model

Table 3.2: Dimensions of the micro-jet heat sink

A_{cs} (mm)	H_c (mm)	t_s (mm)	d_n (mm)	l_n (mm)	S_n (mm)
12×12	0.3	0.1	0.1	0.5	3.5

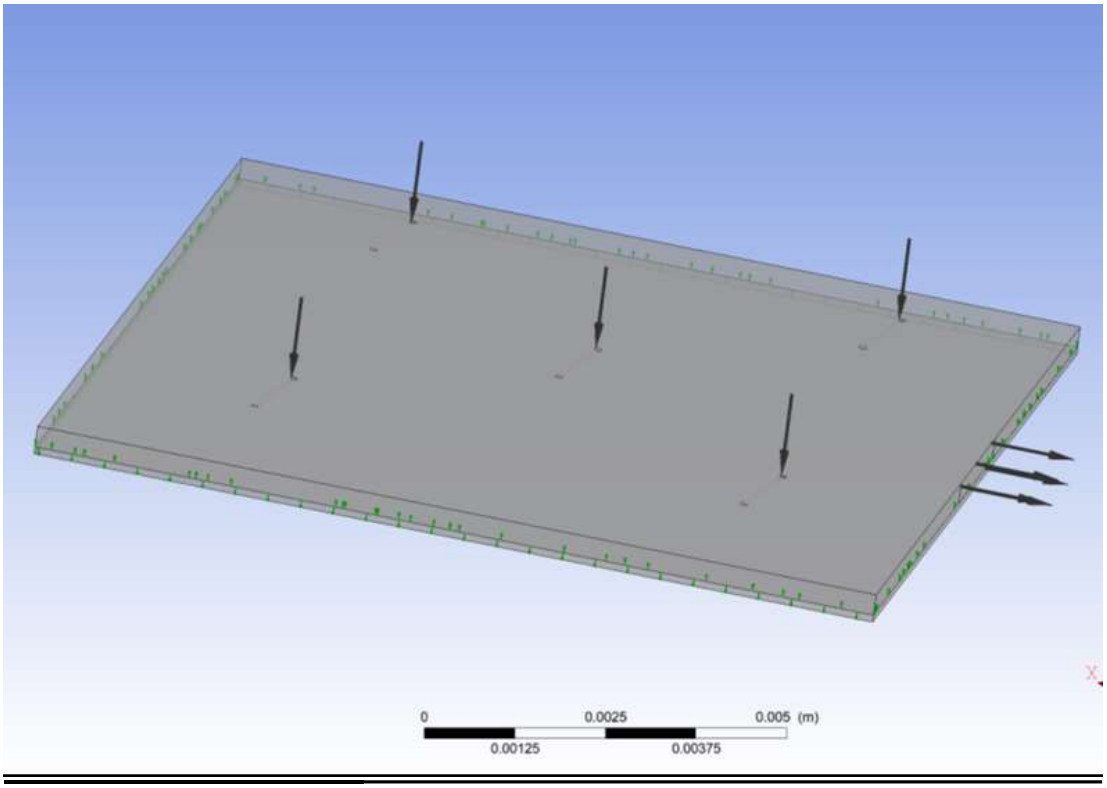

Figure 3.3: Geometry of the 5 micro-jet impingement heat sink.

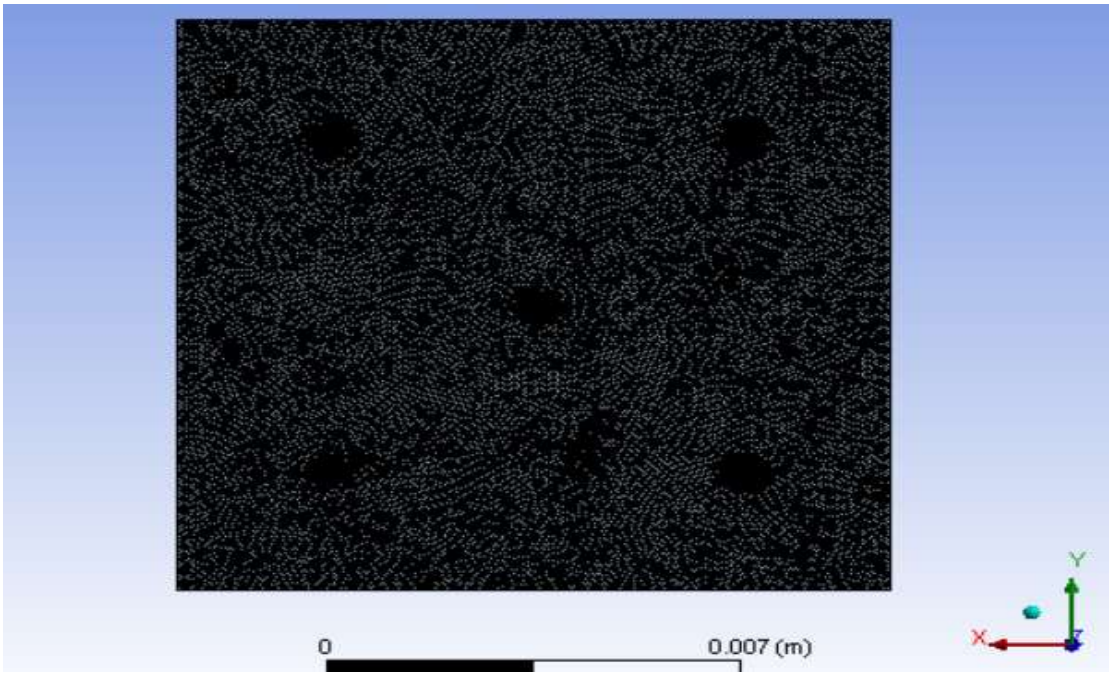

Figure 3.4: Meshing of the 5 micro-jet impingement heat sink in ANSYS CFX.

Mesh details-

Physics preference	CFD
Solver preference	CFX
Use Advanced Size Function	On: Proximity and Curvature
Relevance Center	Coarse
Smoothing	Medium
Transition	Slow
Transition ratio	0.77
Minimum size	Default (8.4707e-006 m)
Maximum face size	Default (8.4707e-004 m)
Maximum size	Default (1.6941e-003 m)
Nodes	1108108
Elements	3400579

Problem 3: Inclined 9 jet model

Table 3.3: Dimensions of the micro-jet heat sink

A_{cs} (mm)	H_c (mm)	t_s (mm)	d_n (mm)	l_n (mm)	S_n (mm)
12×12	0.3	0.1	0.1	0.5	4

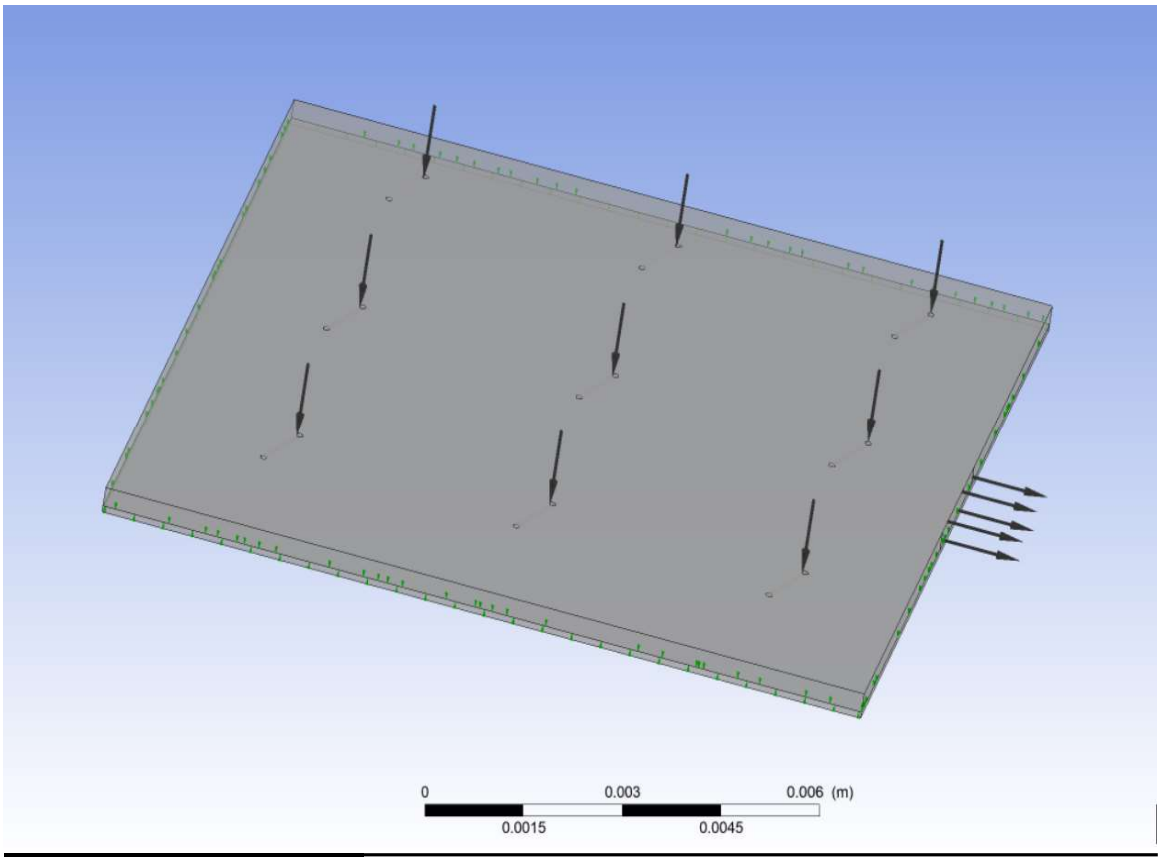

Figure 3.5: Geometry of the 9 micro-jet impingement heat sink.

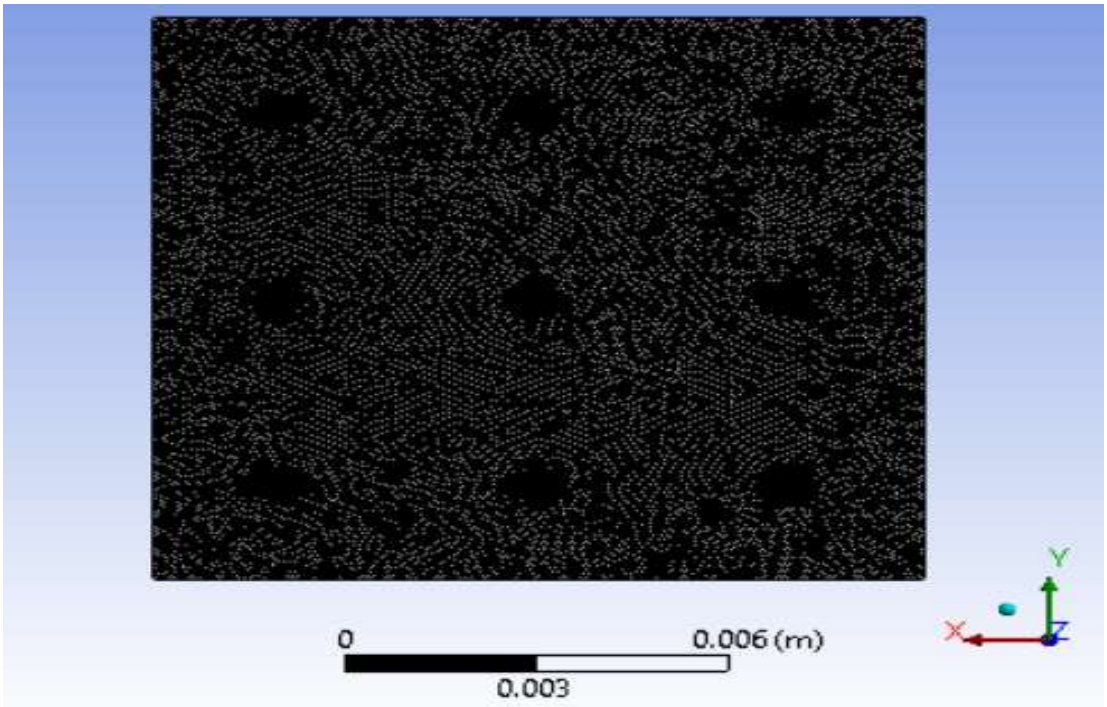

Figure 3.6: Meshing of the 9 micro-jet impingement heat sink in ANSYS CFX.

Mesh details-

Physics preference	CFD
Solver preference	CFX
Use Advanced Size Function	On: Proximity and Curvature
Relevance Center	Coarse
Smoothing	Medium
Transition	Slow
Transition ratio	0.77
Minimum size	Default (8.4707e-006 m)
Maximum face size	Default (8.4707e-004 m)
Maximum size	Default (1.6941e-003 m)
Nodes	852104
Elements	2619805

Problem 4: Inclined 13 jet model

Table 3.4: Dimensions of the micro-jet heat sink

A_{cs} (mm)	H_c (mm)	t_s (mm)	d_n (mm)	l_n (mm)	S_n (mm)
12×12	0.3	0.1	0.1	0.5	2

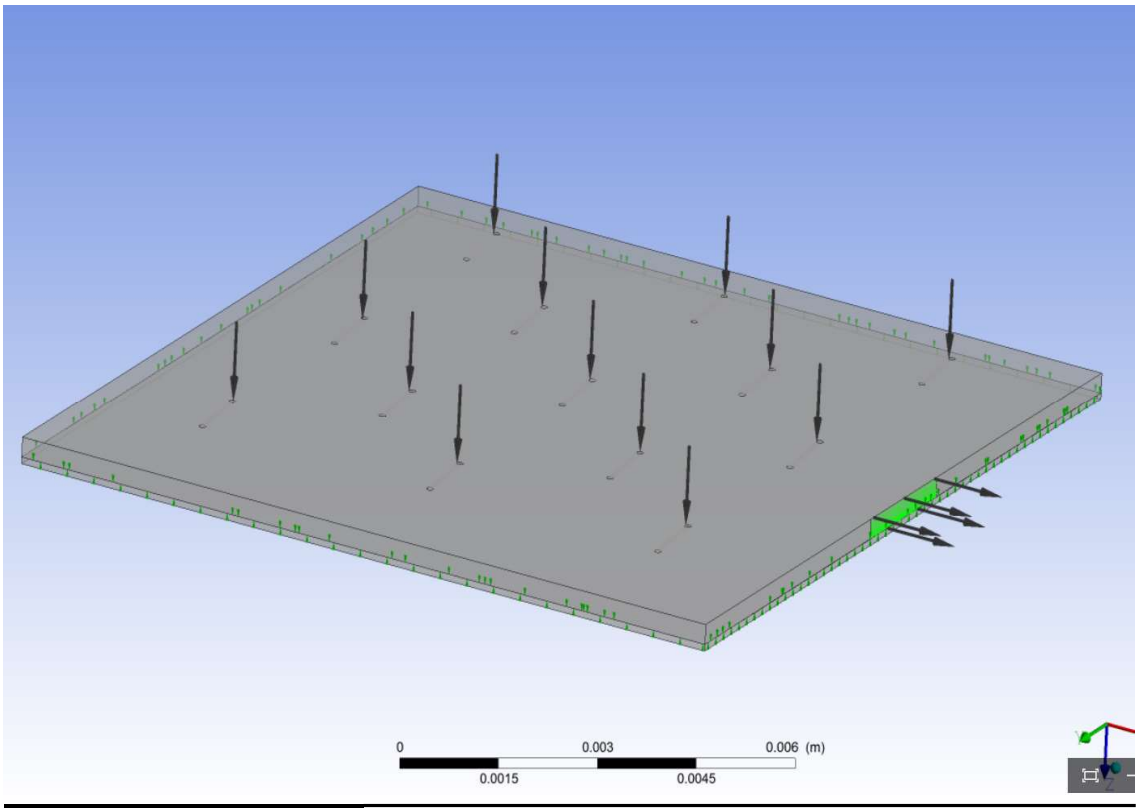

Figure 3.7: Geometry of the 13 micro-jet impingement heat sink.

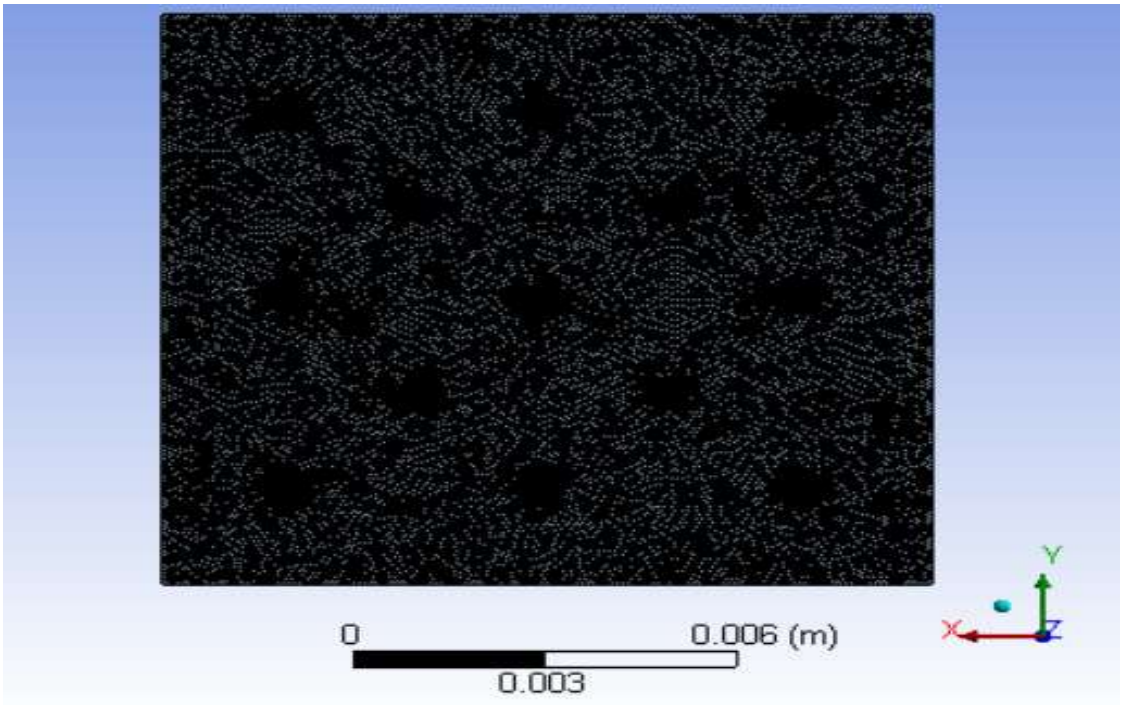

Figure 3.8: Meshing of the 13 micro-jet impingement heat sink in ANSYS CFX.

Mesh details-

Physics preference	CFD
Solver preference	CFX
Use Advanced Size Function	On: Proximity and Curvature
Relevance Center	Coarse
Smoothing	Medium
Transition	Slow
Transition ratio	0.77
Minimum size	Default (8.4707e-006 m)
Maximum face size	Default (8.4707e-004 m)
Maximum size	Default (1.6941e-003 m)
Nodes	1153462
Elements	3622701

Problem 5: Inclined 16 jet model

Table 3.5: Dimensions of the micro-jet heat sink

A_{cs} (mm)	H_c (mm)	t_s (mm)	d_n (mm)	l_n (mm)	S_n (mm)
12×12	0.3	0.1	0.1	0.5	2.4

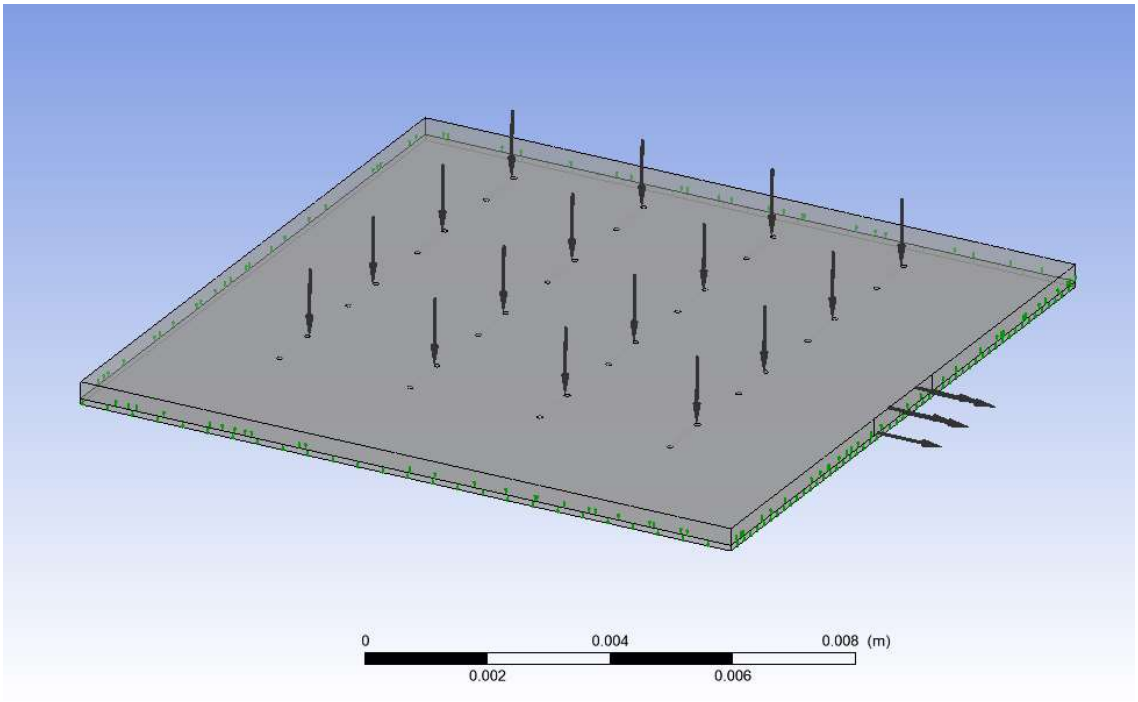

Figure 3.9: Geometry of the 16 micro-jet impingement heat sink.

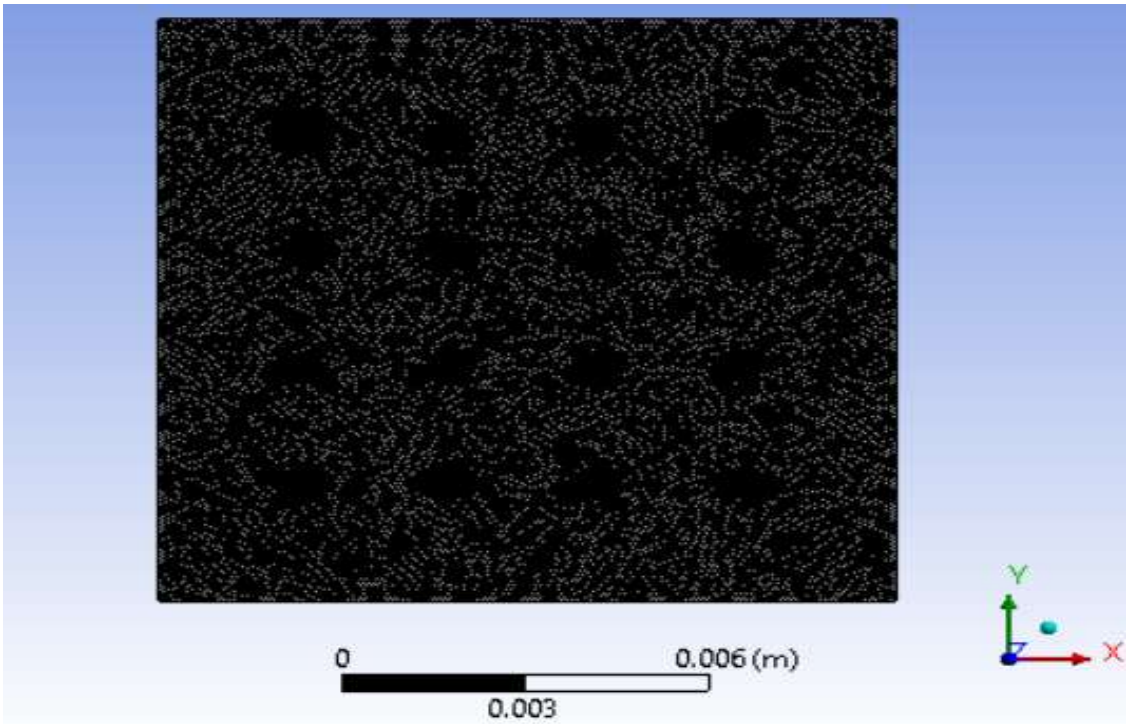

Figure 3.10: Meshing of the 16 micro-jet impingement heat sink in ANSYS CFX.

Mesh details-

Physics preference	CFD
Solver preference	CFX
Use Advanced Size Function	On: Proximity and Curvature
Relevance Center	Coarse
Smoothing	Medium
Transition	Slow
Transition ratio	0.77
Minimum size	Default (8.4707e-006 m)
Maximum face size	Default (8.4707e-004 m)
Maximum size	Default (1.6941e-003 m)
Nodes	890517
Elements	2809000

Set up details-

Before giving the boundary conditions two domains were created in the ANSYS CFX set up. Out of the two domains created one domain was given the name as fluid while the other domain was assigned the name as solid domain. The fluid channel constructed in solid works was given the name fluid domain while the heat sink constructed in solid works was given the name solid domain.

After making the domains in the set up the boundary conditions were created in the solid domain and the fluid domain. Inlet and outlet boundary conditions were given in the fluid domain whereas the bottom wall heat flux and adiabatic conditions for the remaining walls were given in the solid domain.

Table 3.6: Zone specification

Heat sink front wall	adiabatic
Heat sink top wall	adiabatic
Heat sink back wall	adiabatic
Heat sink bottom wall	Heat flux in
Heat sink right wall	adiabatic
Heat sink left wall	adiabatic
Channel entry	Static pressure
Channel outlet	Mass flow outlet
Default Interface	Conservative heat transfer

Table 3.7: Solver settings

Following are the solver settings which are to be used in simulation.

Min. Iterations	1
Max. Iterations	100
Residual type	RMS
Residual target	1E-4
Time scale control	Auto time scale

CHAPTER-4

VALIDATION

In this computational analysis validation is done for inclined (45□ degree) micro-jet impingement heat sink and the results are plotted for maximum temperature drop and maximum pressure drop in inclined micro-jet heat sink for different values of heat fluxes applied at the bottom surface of the heat sink for a set value of mass flow rate. Four values of heat flux used in the validation which are 5,10,15 and 20 W/cm^2.

The grid meshing test was carried out for both solid and liquid domains in CFX and a meshing of approximately 3568577 elements was used for a particular design of; $\alpha = 3$, inclined 4 micro-jet-array. The changes in pressure variation and maximum temperature-drop were less than 3 to 4 % for meshing grid of 1129108 nodes and 3568577 elements.The validation of the present scheme was carried out for a laminar flow of fluid into the micro-jet. The validation results were compared with the experimental results reported in [32]. In the real validation analysis the outer surface of the fluid domain and solid domain are subjected to heat loss to the surrounding air by natural convection and radiation. In the present validation and simulation analysis the heat loss by natural convection was found to be less than one percent on the thermal performance of the model, hence it can be ignored safely and also for simplicity of the model, radiation heat loss are also ignored in present investigation.

4.1 Experimental model: Straight jet

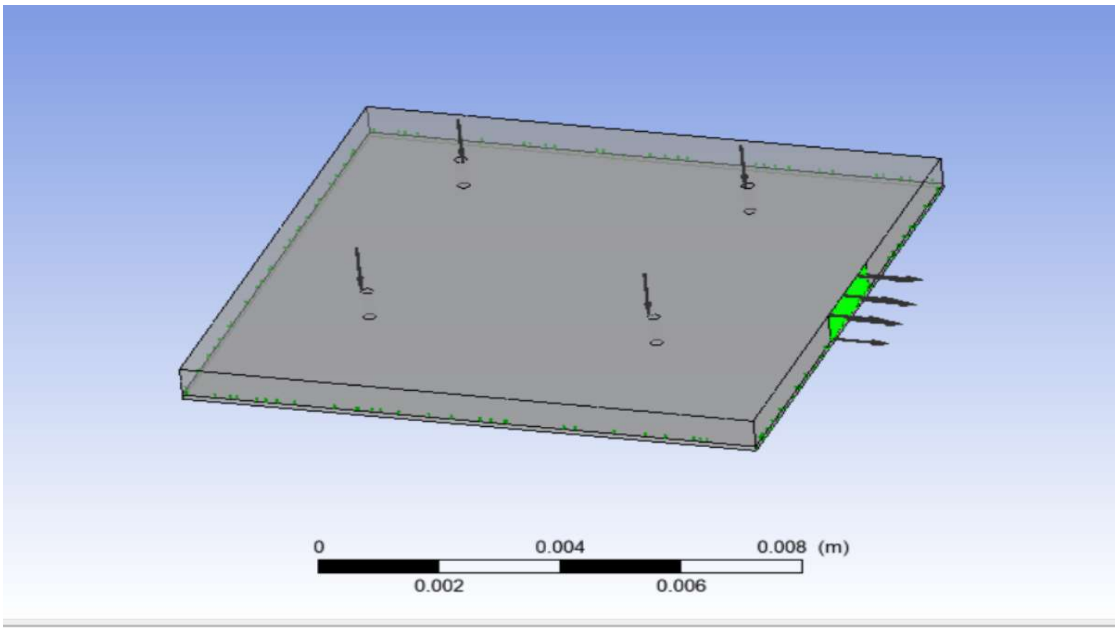

Figure 4.1: Geometry of straight jet impingement heat sink used in validation.

Results for above model at different heat flux values:

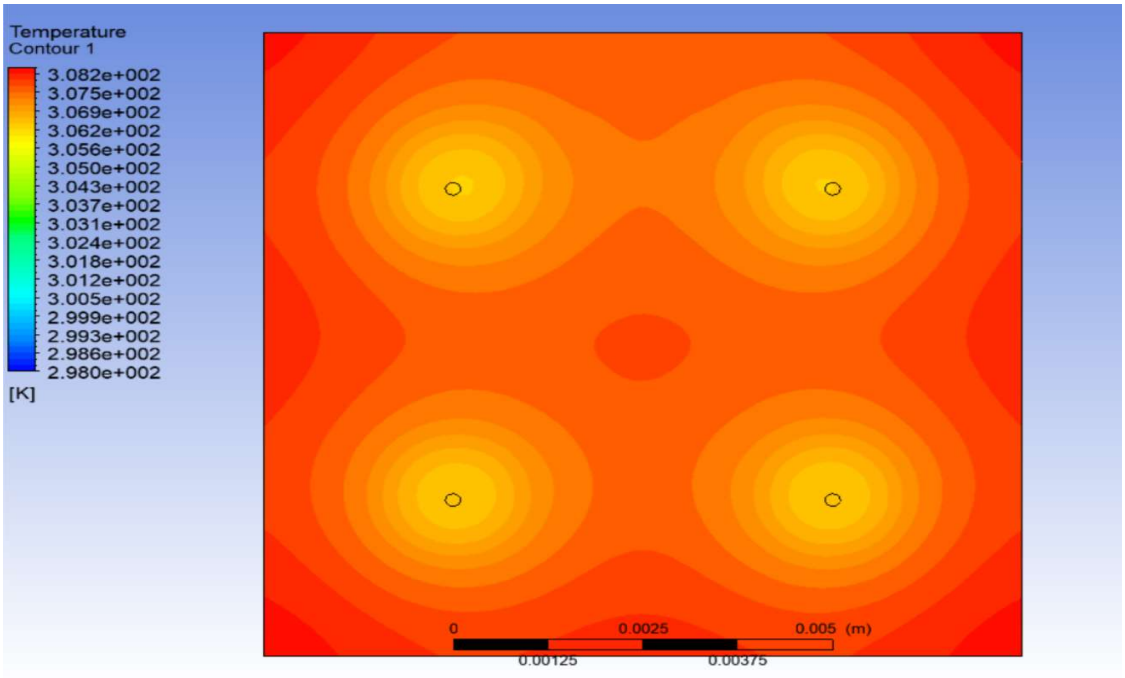

Figure 4.2: Temperature contour at solid-fluid interface at heat flux = 5 W/cm^2.

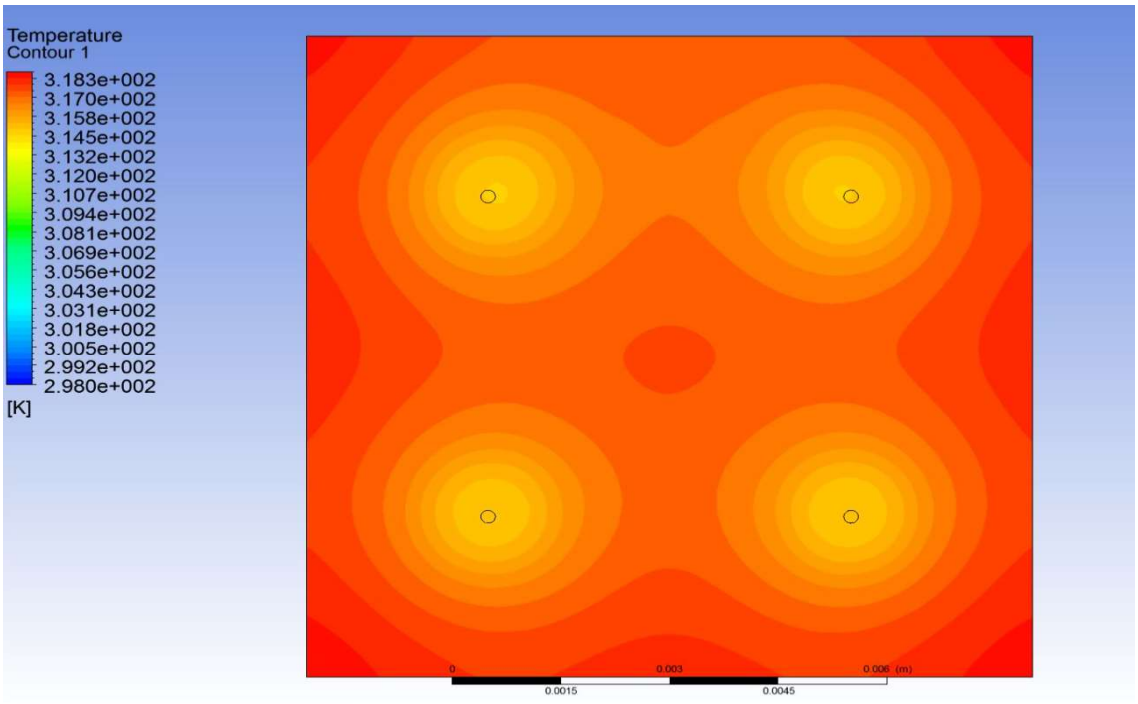

Figure 4.3: Temperature contour at solid-fluid interface at heat flux = 10 W/cm^2.

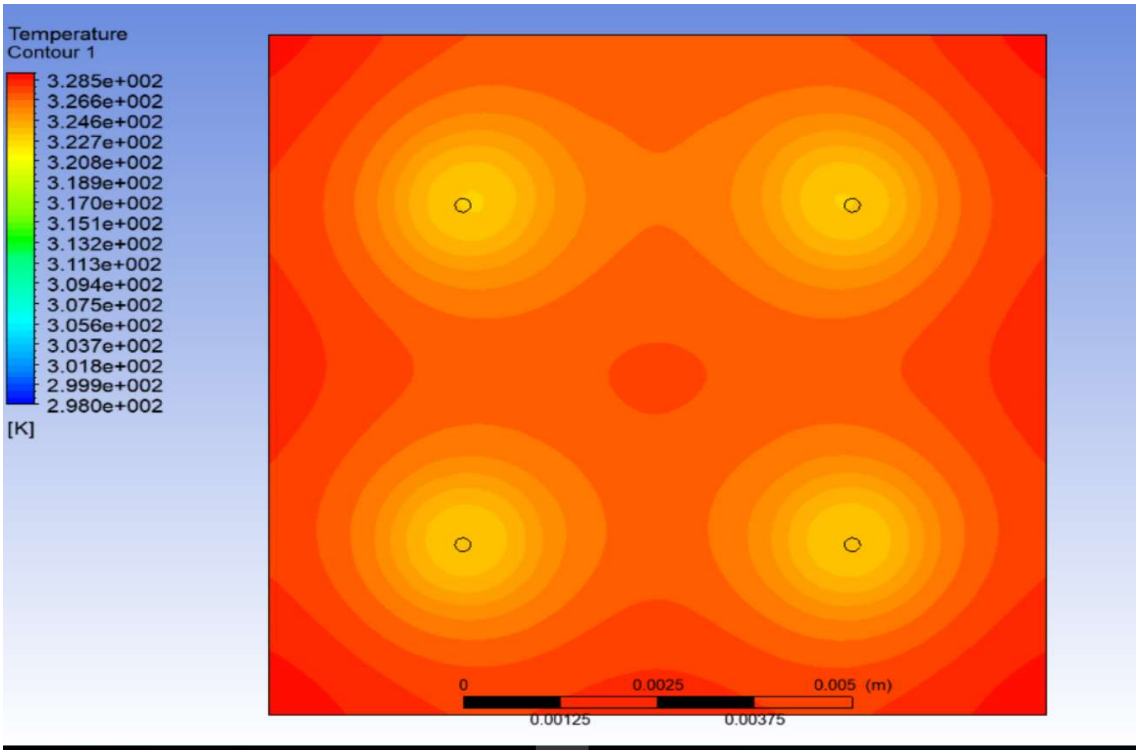

Figure 4.4: Temperature contour at solid-fluid interface at heat flux = 15 W/cm^2.

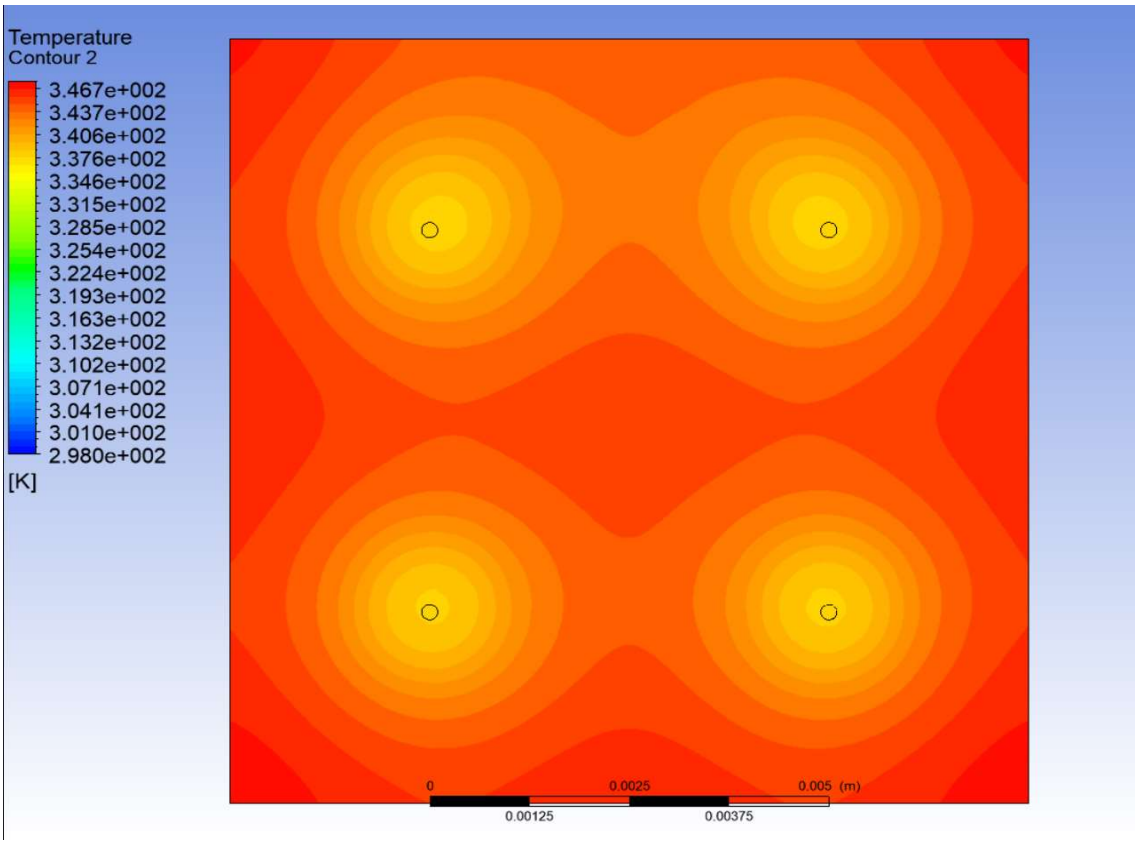

Figure 4.5: Temperature contour at solid-fluid interface at heat flux = 20 W/cm^2.

- Figure 4.2, 4.3, 4.4 & 4.5 show the Temperature contours at solid-fluid interface across channel for straight jet impingement heat sink at heat flux values of 5,10,15& 20 W/cm^2 respectively where the mass flow rate is constant =0.000122 kg/s.
- The outlet bulk mean temperature of cooling fluid for Figure 4.2, 4.3, 4.4, & 4.5 are 303 K, 308.3 K, 319.5 K & 336 K respectively.
- The maximum wall Temperature of the base of solid domain are 308 K, 318.3 K , 328.5 K & 346.7 K respectively.

4.2 Present model: Inclined jet (45^{θ})

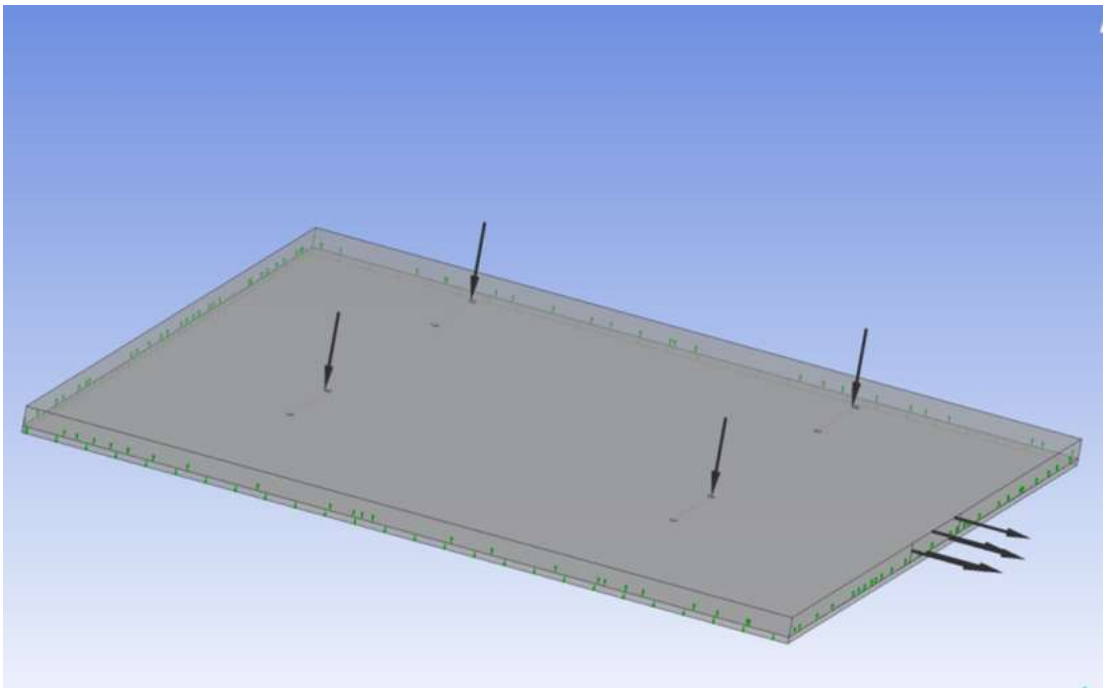

Figure 4.6: Geometry of inclined jet impingement heat sink used in validation.

Results for above model at different heat flux values:

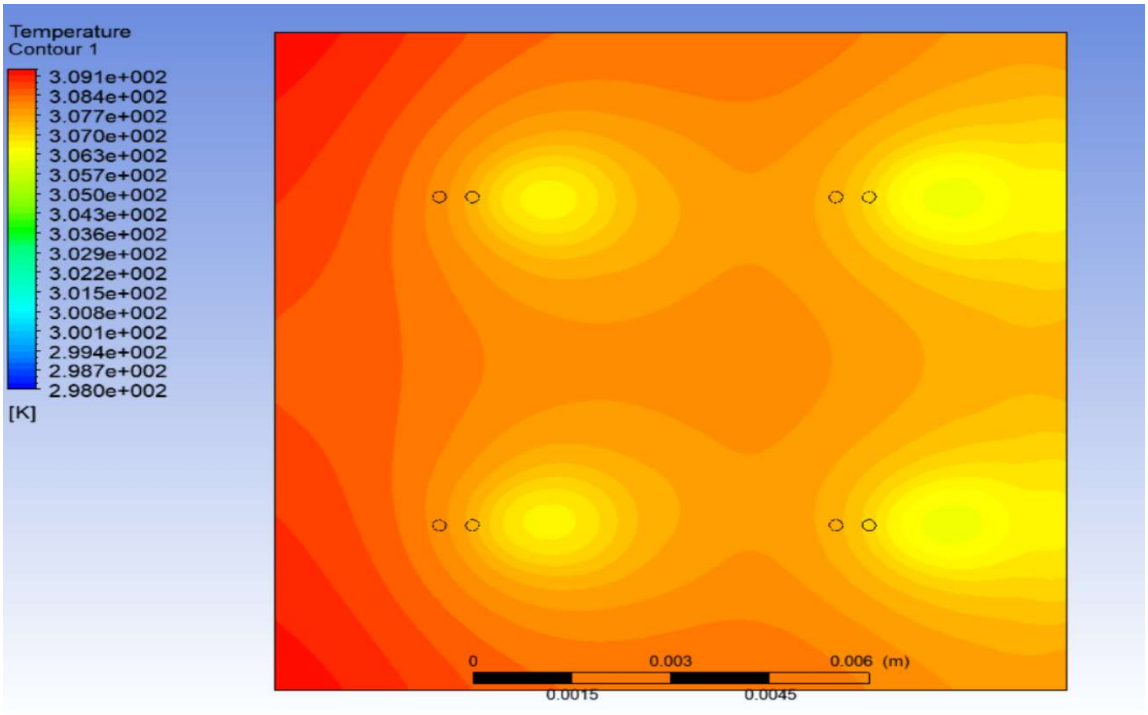

Figure 4.7: Temperature contour at solid-fluid interface at heat flux = 5 W/cm^2.

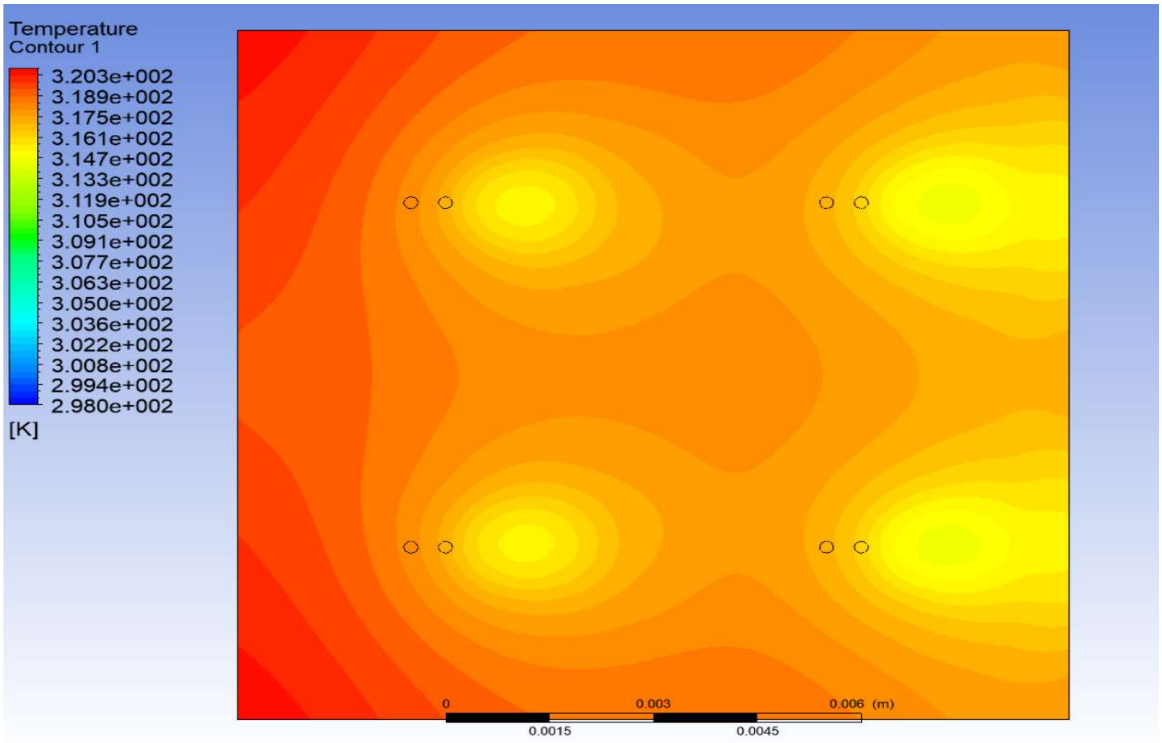

Figure 4.8: Temperature contour at solid-fluid interface at heat flux = 10 W/cm^2.

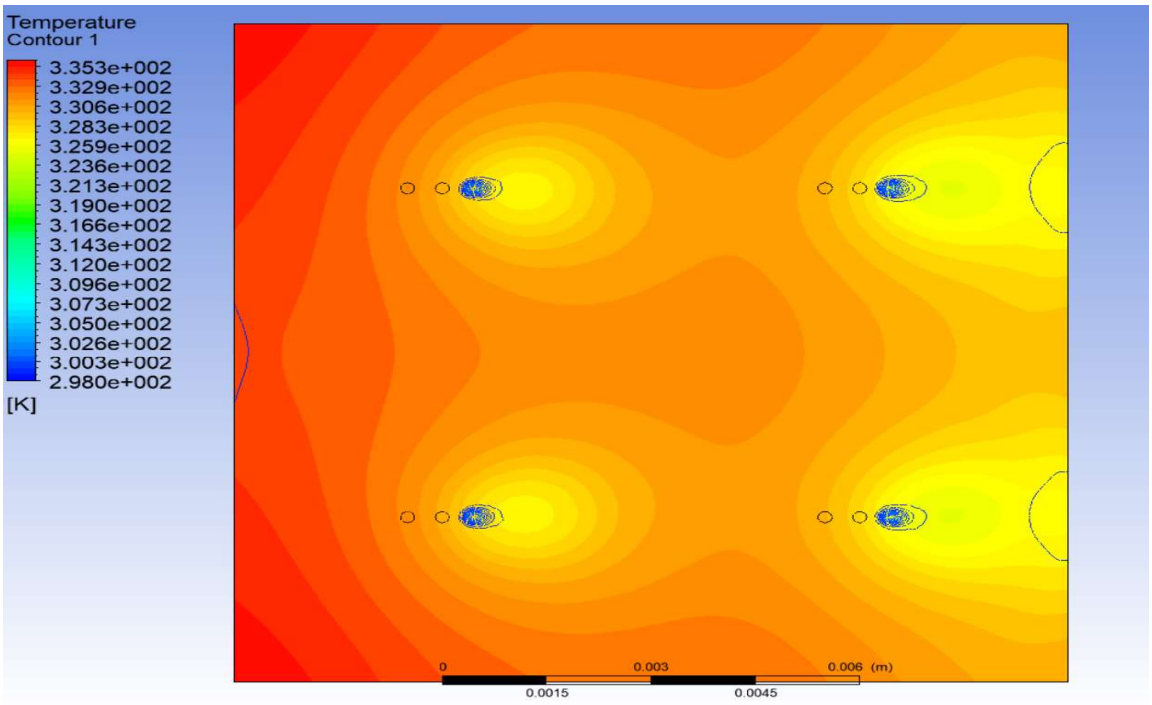

Figure 4.9: Temperature contour at solid-fluid interface at heat flux = 15 W/cm^2.

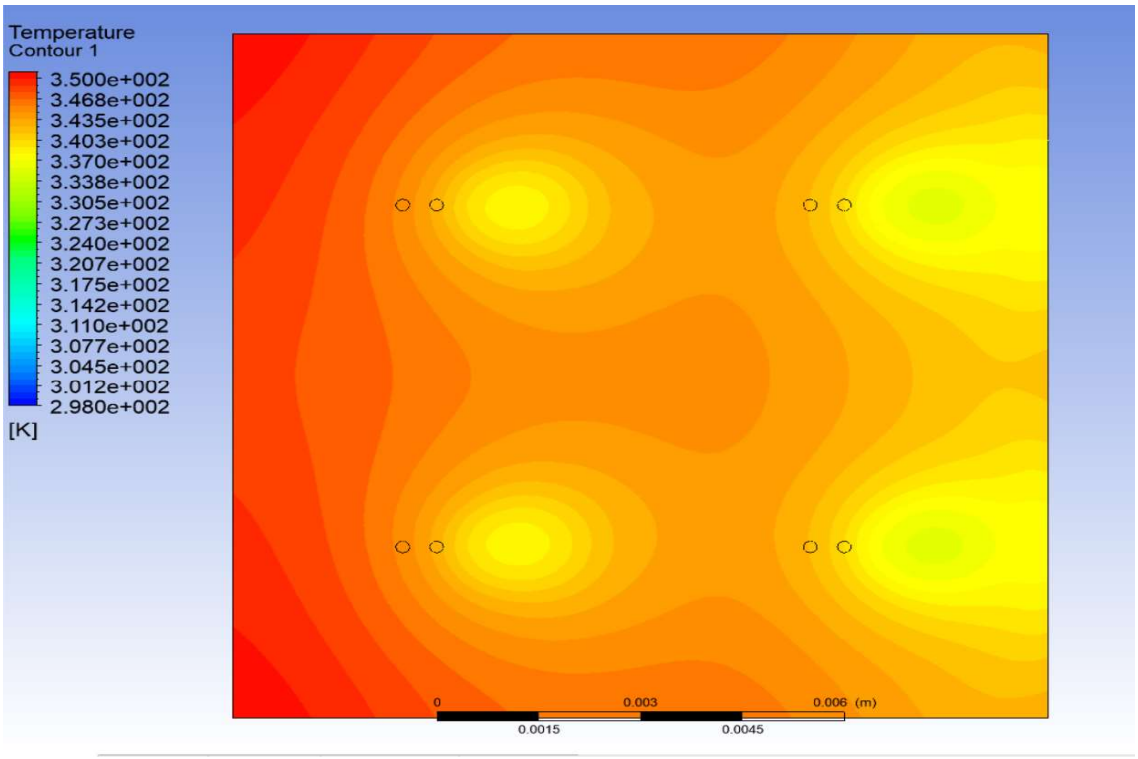

Figure 4.10: Temperature contour at solid-fluid interface at heat flux= 20 W/cm^2.

- Figure 4.7, 4.8, 4.9 & 4.10 show the Temperature contours at solid-fluid interface across channel for inclined jet impingement heat sink at heat flux values of 5,10,15 & 20 W/cm^2 respectively where the mass flow rate is constant =0.000122 kg/s.
- The outlet temperature of cooling fluid for Figure 4.7, 4.8, 4.9 & 4.10 are 303.6 K, 310 K, 325.3 K & 342 K respectively.
- The maximum wall Temperature of the base of solid domain are 309.1 K, 320.3 K , 335.3 K & 350 K respectively.

Table 4: Values of maximum temperature rise of cooling fluid

Heat flux (W/cm^2)	ΔT_{max} [K] Experimental	ΔT_{max} [K] present
5	5	5.6
10	10.3	12
15	21.5	27.3
20	38	44

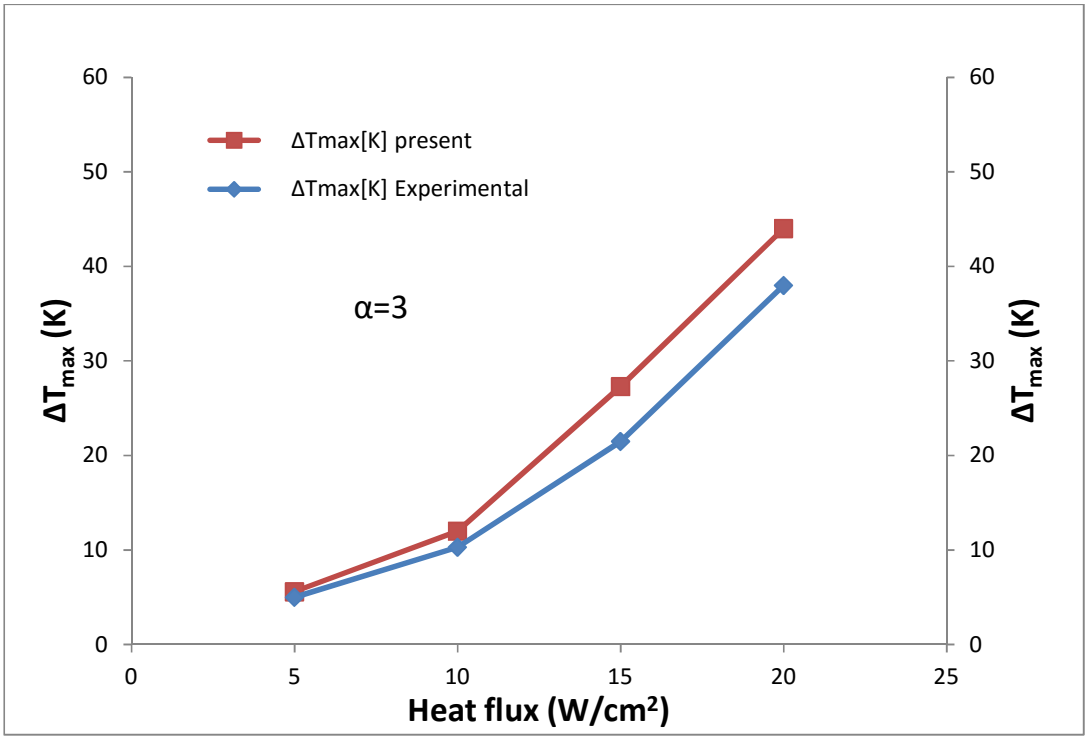

Fig. 4.11 Validation of the present model results in comparison with the experimental model results reported by [29].

CHAPTER-5

SIMULATION RESULTS

Simulation results for different no. of micro-jets in a rectangular impingement heat sink

In the following computational fluid dynamics analysis the results are plotted for temperature drop of the heated surface and pressure drop across the channel in different no. of impingement jets in a rectangular heat sink for a set value of heat flux applied at the bottom wall of the heat sink. Where mass flow rate is being kept constant. The value of heat flux used in the analysis are 150 W/cm^2. The thermal performance of the different jet configurations, i.e. inclined 4 jet, staggered 5-jet, 9 jet, 13-jet and 16 jet arrays were analyzed for the maximum heat transfer rate, maximum temperature drop and pressure variation at a constant flow rate ie 1.22×10^{-4} kg/s^{-1}, for $\alpha = 3$, $\alpha = 2$ and $\alpha = 1.5$, where α is a design parameter which is defined as the ratio of height of the fluid channel, H_c & the nozzle diameter, d_n i.e. $\alpha = H_c / d_n$.

5.1 Results for 4 micro-jets impingement heat sink with different nozzle diameter :

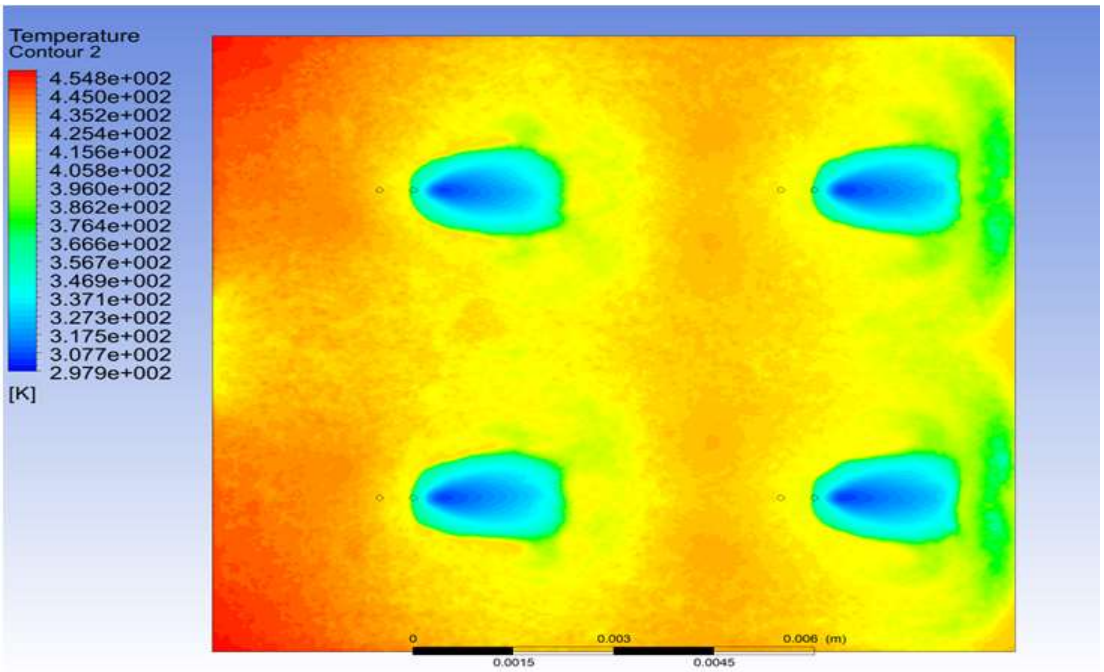

Figure 5.1: Temperature contour at solid-fluid interface across channel for 4 jet at $\alpha = 3$.

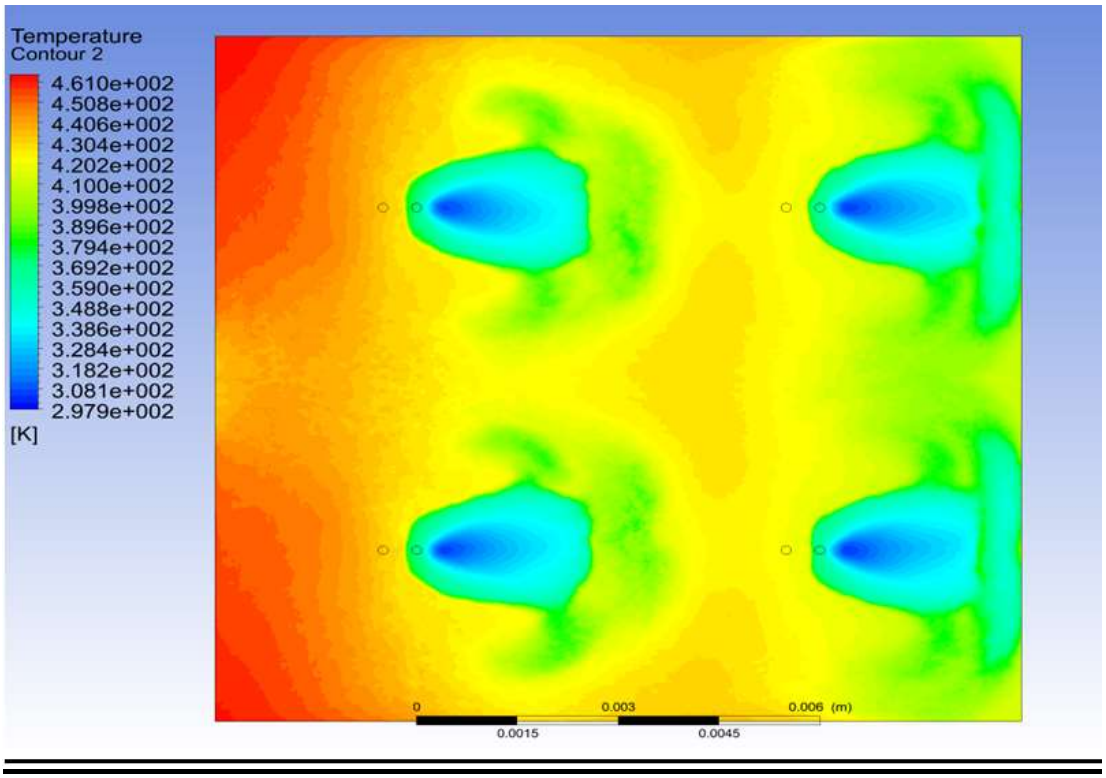

Figure 5.2: Temperature contour at solid-fluid interface across channel for 4 jet at α = 2.

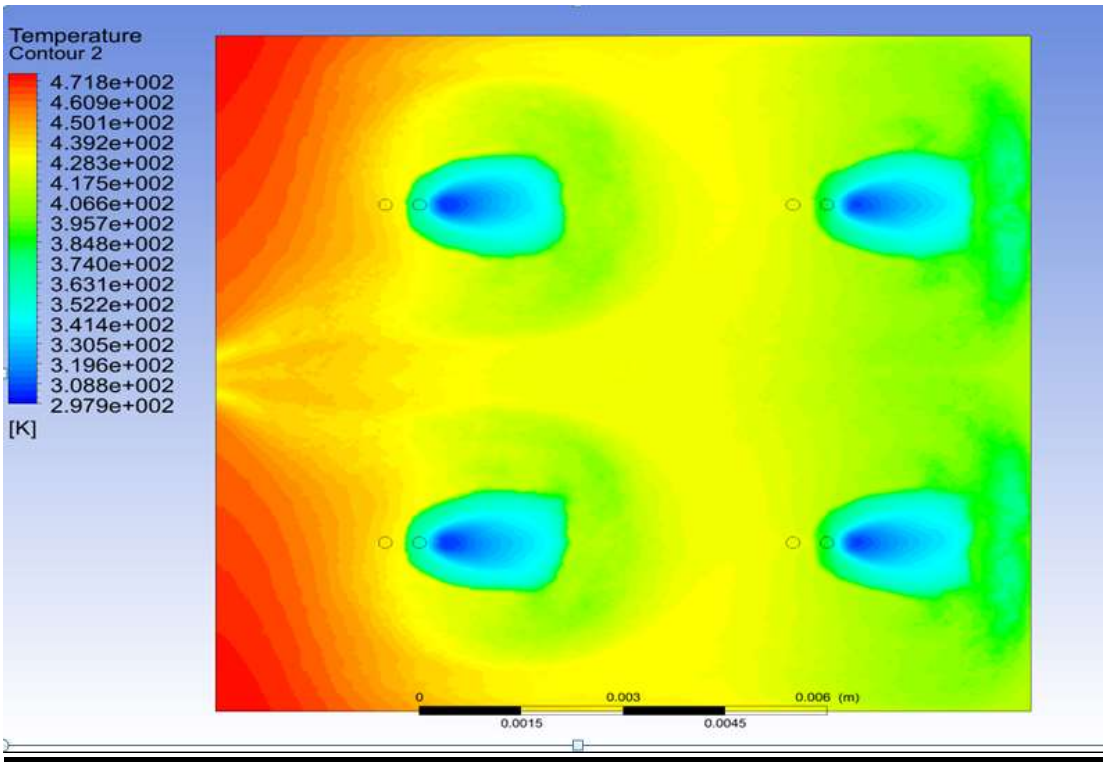

Figure 5.3: Temperature contour at solid-fluid interface across channel for 4 jet at α = 1.5.

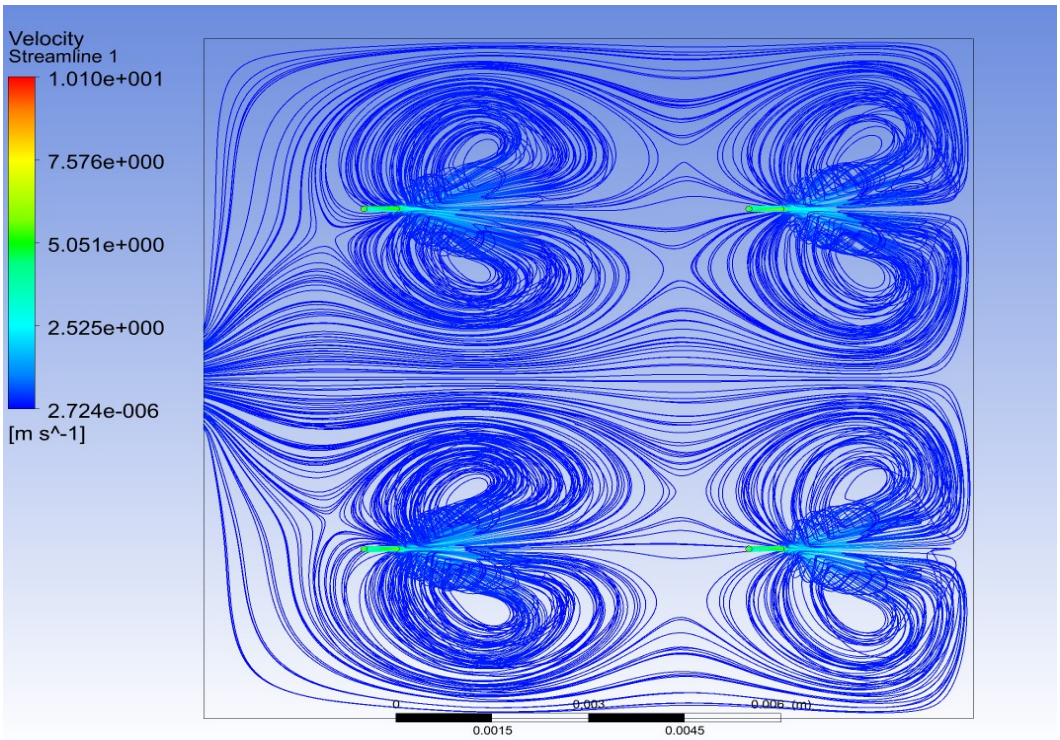

Figure 5.4: Velocity contour at solid-fluid interface across channel for 4 jet at α = 3.

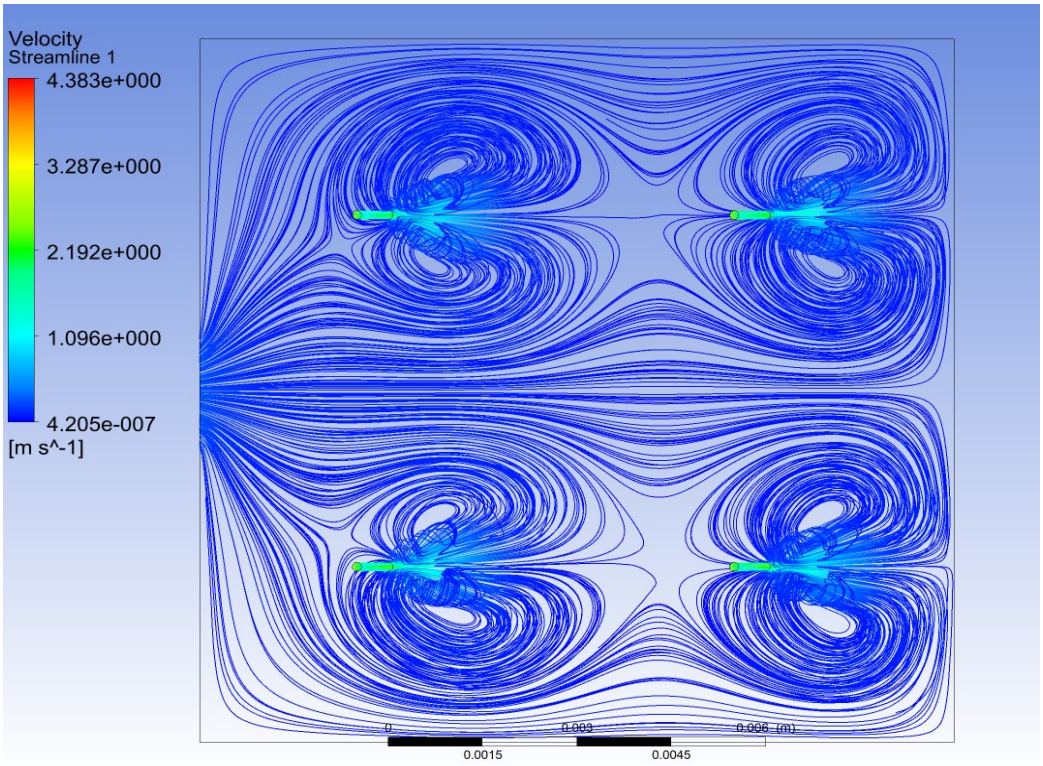

Figure 5.5: Velocity contour at solid-fluid interface across channel for 4 jet at α = 2.

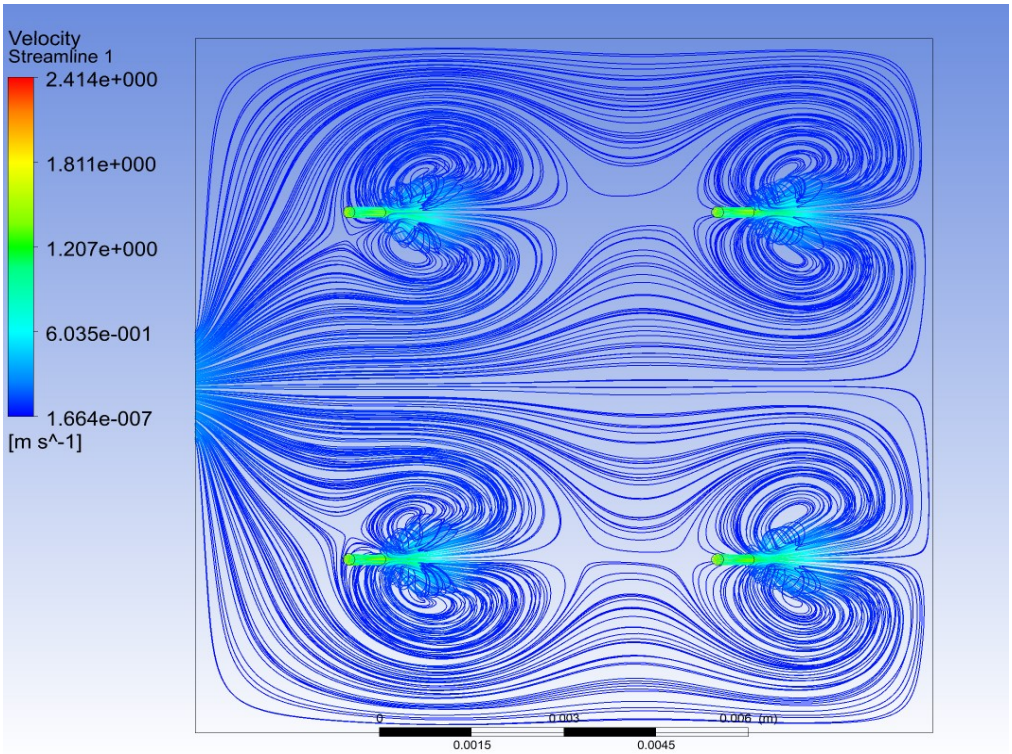

Figure 5.6: Velocity contour at solid-fluid interface across channel for 4 jet at α = 1.5.

- The above figure 5.4, fig 5.5 & fig 5.6 shows velocity contour at solid-fluid interface across channel in a 4 jet impingement heat sink for α = 3, α = 2 & α = 1.5 respectively.
- As the diameter of nozzle increase velocity of the fluid decreases shown in fig 5.4, 5.5 & 5.6 since mass flow rate is constant.
- the stream line pattern obtained in velocity contours are same in all the remaining jet configuration.
- In figure 5.1 the average surface Temperature of fluid-solid interface is 434.8 K.
- In figure 5.2 the average surface Temperature of fluid-solid interface is 440.2 K.
- In figure 5.3 the average surface Temperature of fluid-solid interface is 449.6 K.
- In figure 5.3 Maximum wall temperature is at the bottom wall of the heat sink and is found to be 471.8 K and further the wall temperature increases with increase in nozzle diameter.

Table 5.1: Simulation results for 4 micro-jet heat sink

Design variable $\alpha = H_c / d_n$	average surface Temperature of fluid-solid interface T_{avg} (K)	Bulk mean Temperature of fluid at outlet, T_{b2} (K)	Max pressure drop across the channel ΔP (kpa)
$\alpha = 3$	434.8	338.2	71.89
$\alpha = 2$	440.2	337	21.33
$\alpha = 1.5$	449.6	335.8	7.035

5.2 Results for 5 micro-jets impingement heat sink with different nozzle diameter:

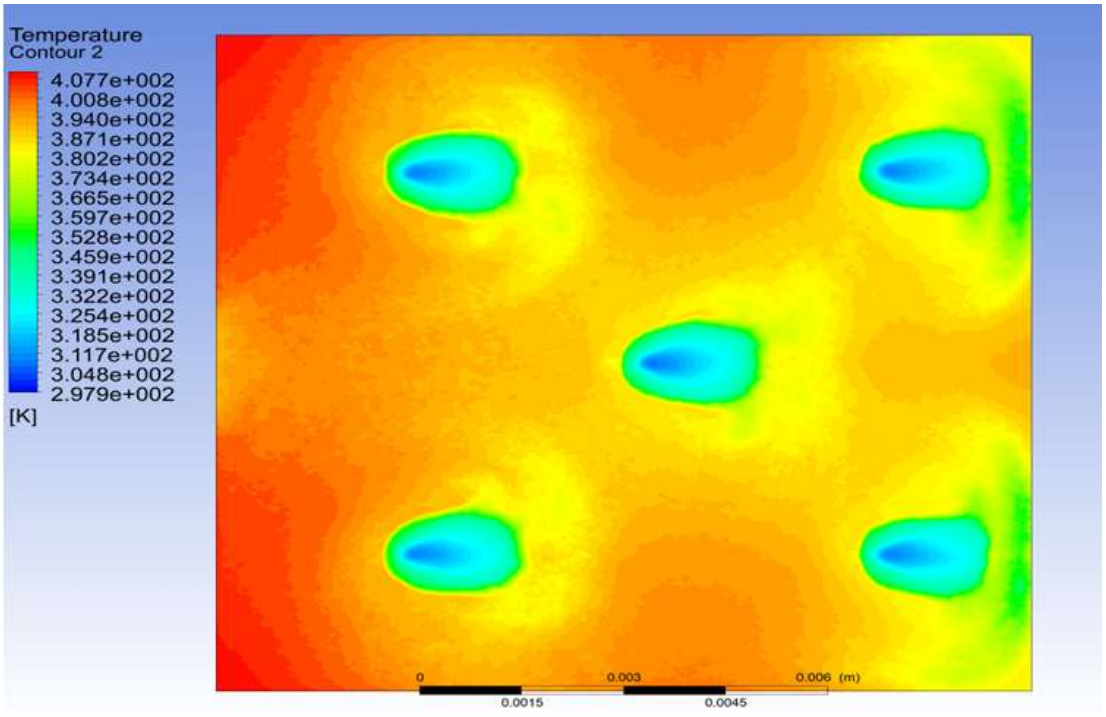

Figure 5.7: Temperature contour at solid-fluid interface across channel for 5 jet at $\alpha = 3$.

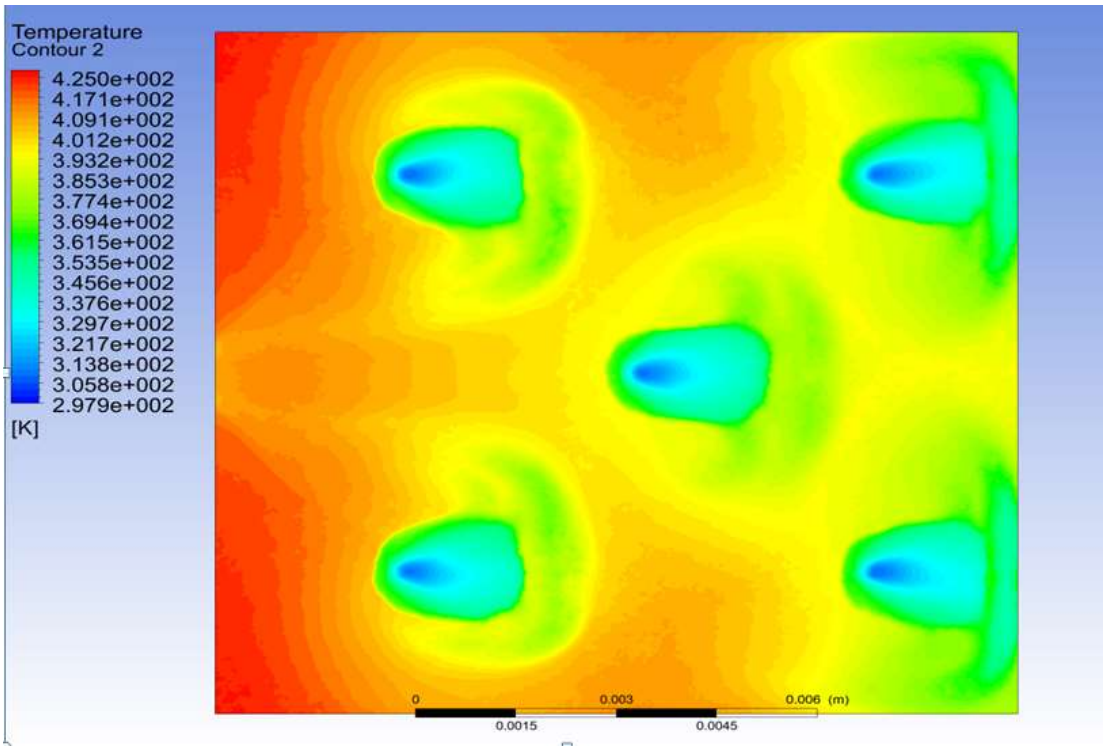

Figure 5.8: Temperature contour at solid-fluid interface across channel for 5 jet at α = 2.

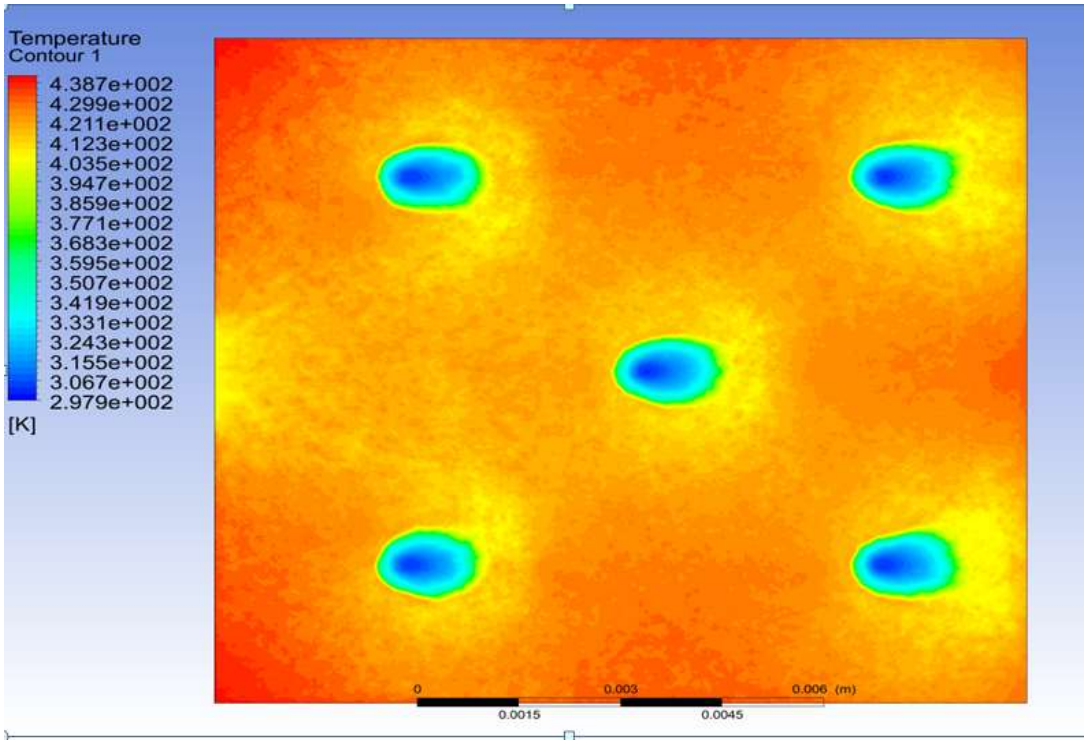

Figure 5.9: Temperature contour at solid-fluid interface across channel for 5 jet at α = 1.5.

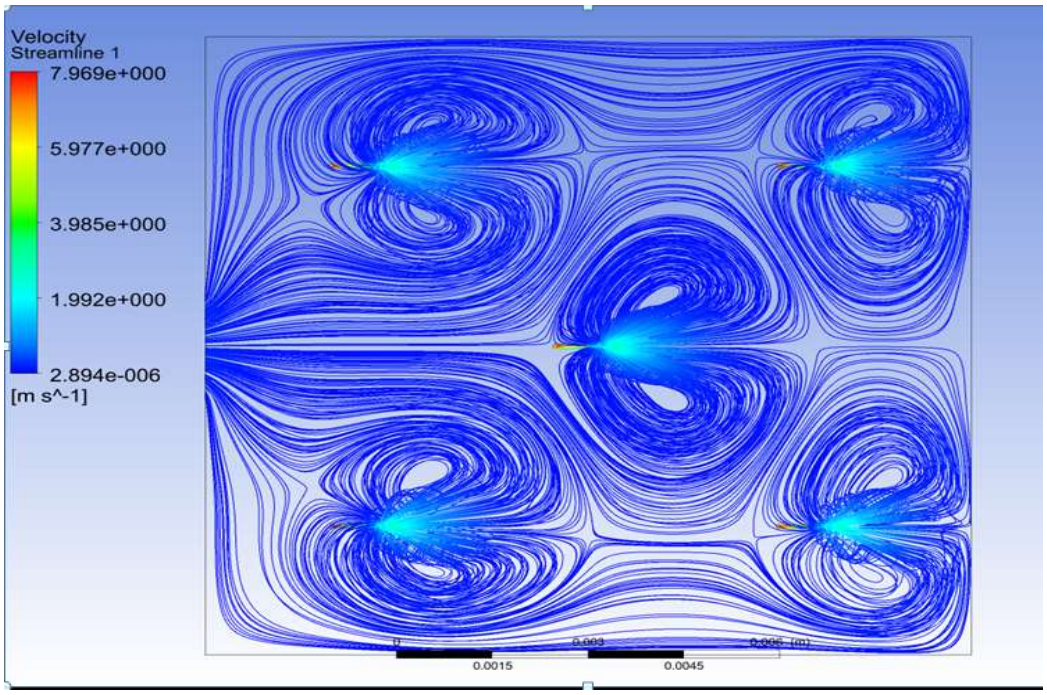

Figure 5.10: Velocity contour at solid-fluid interface across channel for 5 jet at α = 3.

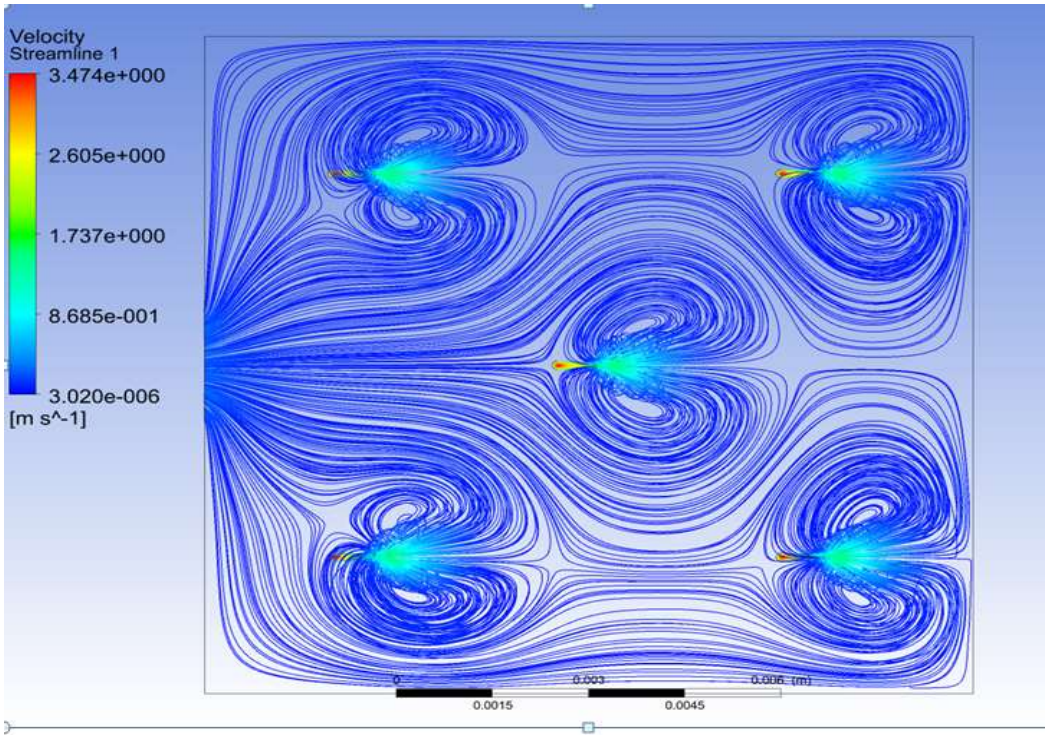

Figure 5.11: Velocity contour at solid-fluid interface across channel for 5 jet at α = 2.

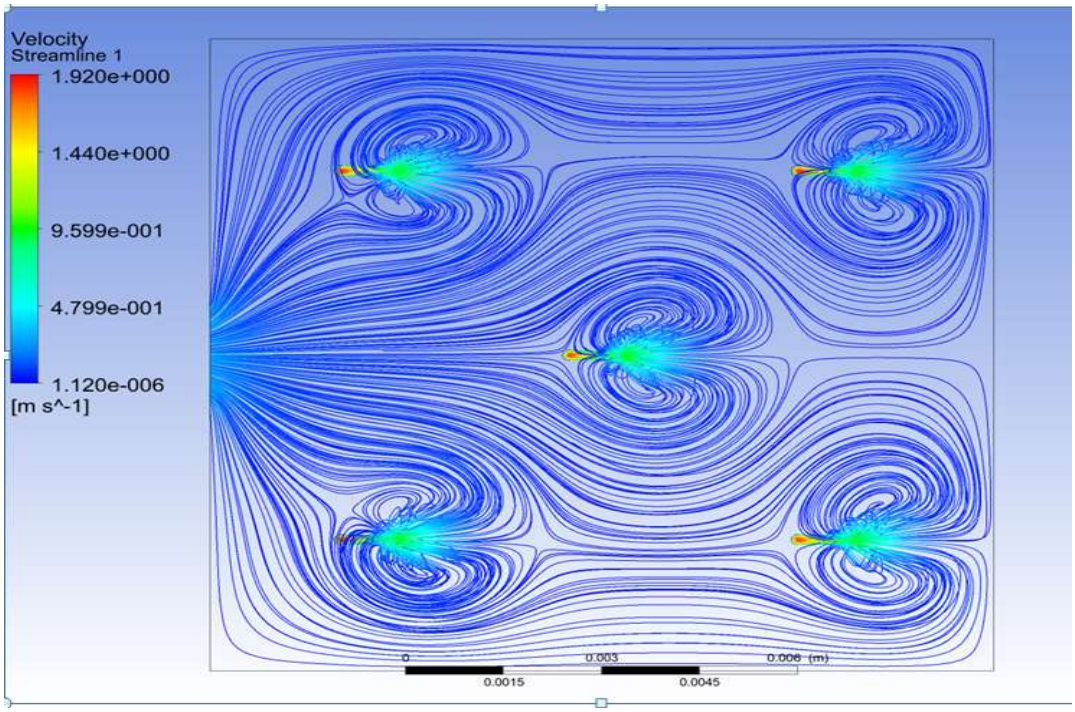

Figure 5.12: Velocity contour at solid-fluid interface across channel for 5 jet at α = 1.5.

- In figure 5.7 the average surface Temperature of fluid-solid interface is 393.6 K.
- In figure 5.8 the average surface Temperature of fluid-solid interface is 409 K.
- In figure 5.9 the average surface Temperature of fluid-solid interface is 420.6 K.
- In figure 5.9 Maximum wall temperature is at the bottom wall of the heat sink and is found to be 438.7 K and further the wall temperature increases with increase in nozzle diameter.

Table 5.2: Simulation results for 5 micro-jet heat sink

Design variable $\alpha = H_c / d_n$	**average surface Temperature of fluid-solid interface** T_{avg} **(K)**	**Bulk mean Temperature of fluid at outlet,** T_{b2} **(K)**	**Max pressure drop across the channel ΔP (kpa)**
α = 3	393.6	346.8	48.08
α = 2	409	343	14.623
α = 1.5	420.6	341.6	4.738

5.3 Results for 9 micro-jets impingement heat sink with different nozzle diameter :

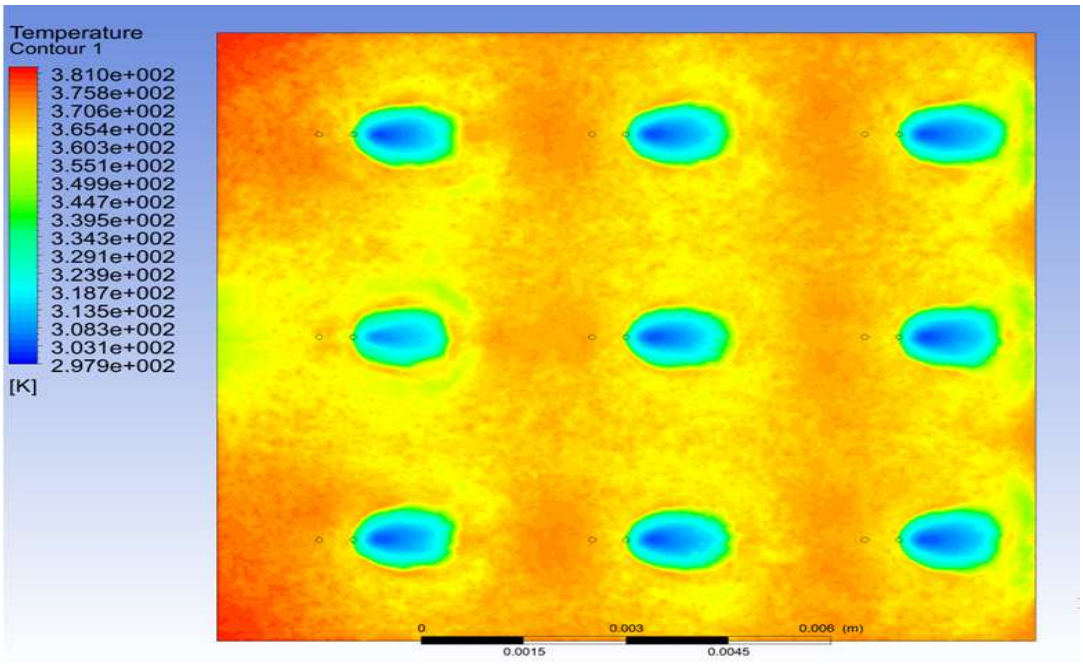

Figure 5.13: Temperature contour at solid-fluid interface across channel for 9 jet at α = 3.

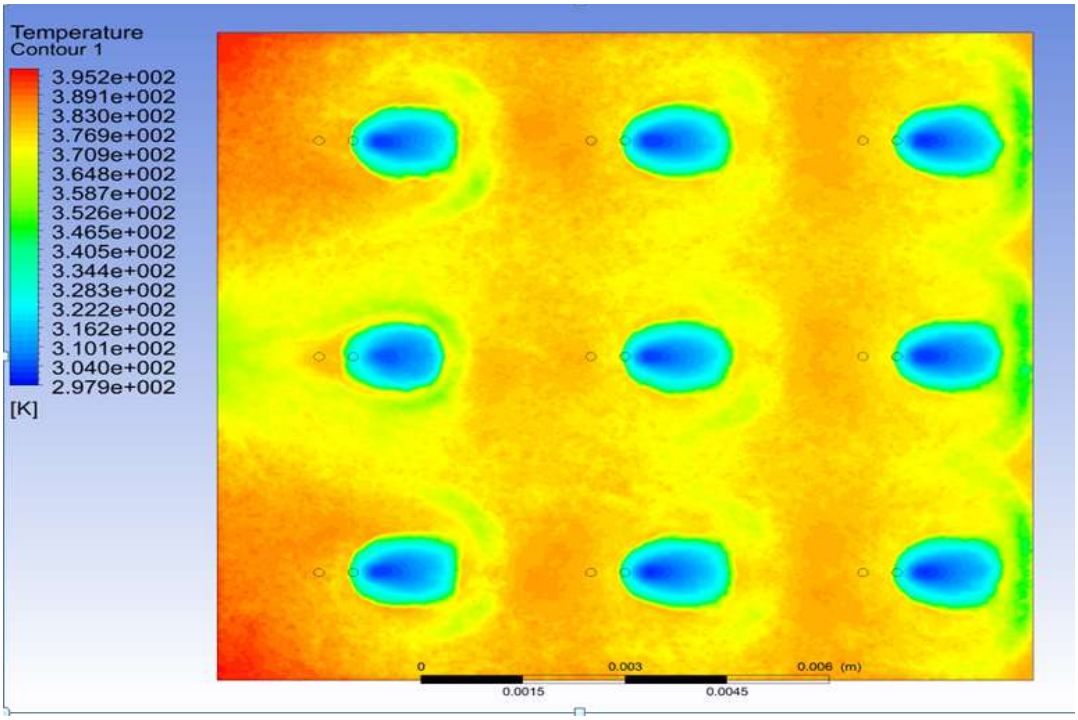

Figure 5.14: Temperature contour at solid-fluid interface across channel for 9 jet at α = 2.

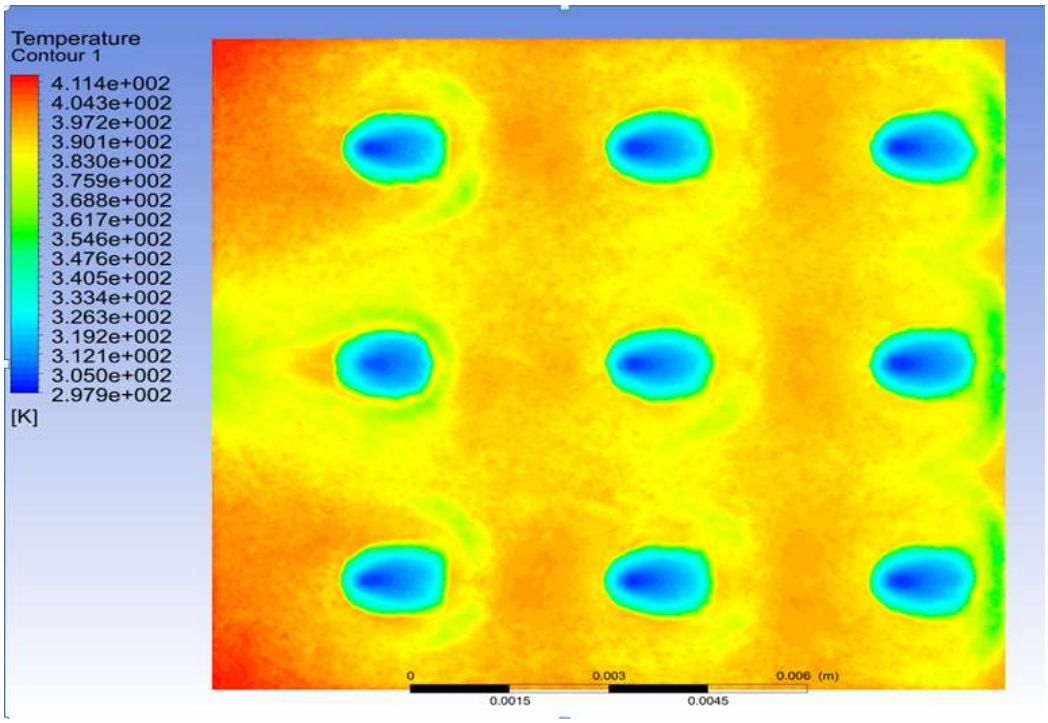

Figure 5.15: Temperature contour at solid-fluid interface across channel for 9 jet at α = 1.5.

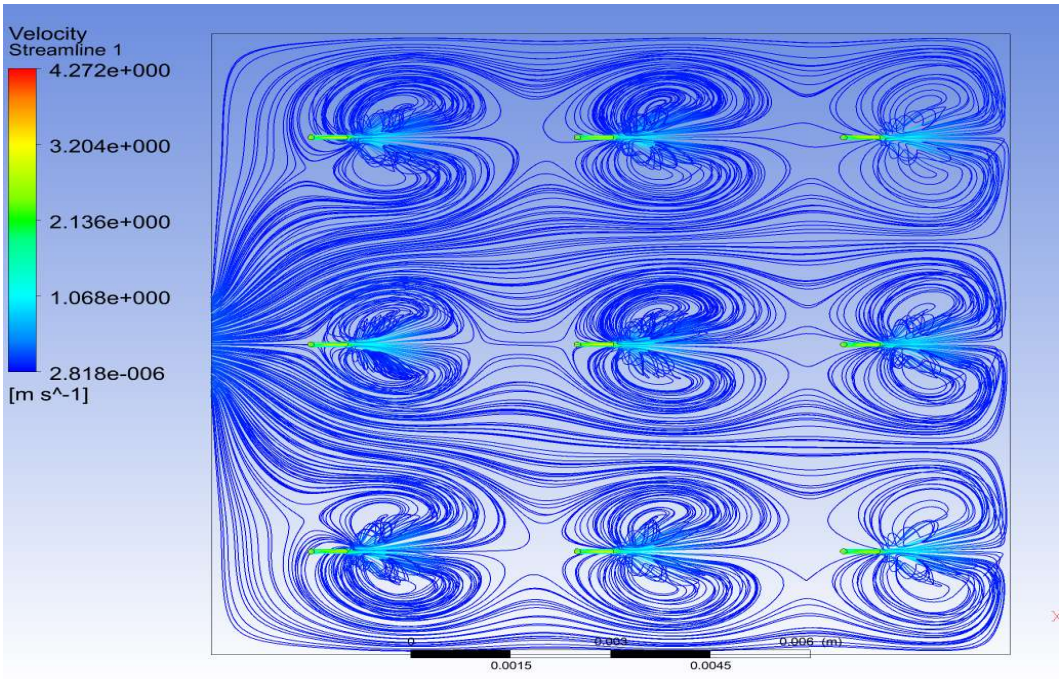

Figure 5.16: Velocity contour at solid-fluid interface across channel for 9 jet at α = 3.

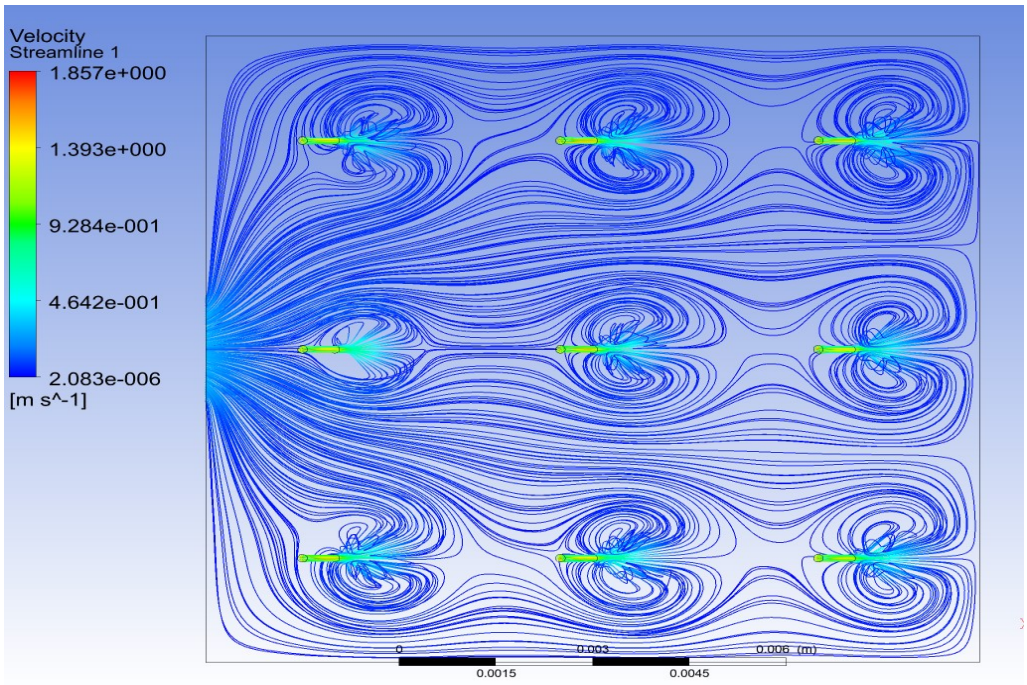

Figure 5.17: Velocity contour at solid-fluid interface across channel for 9 jet at α = 2.

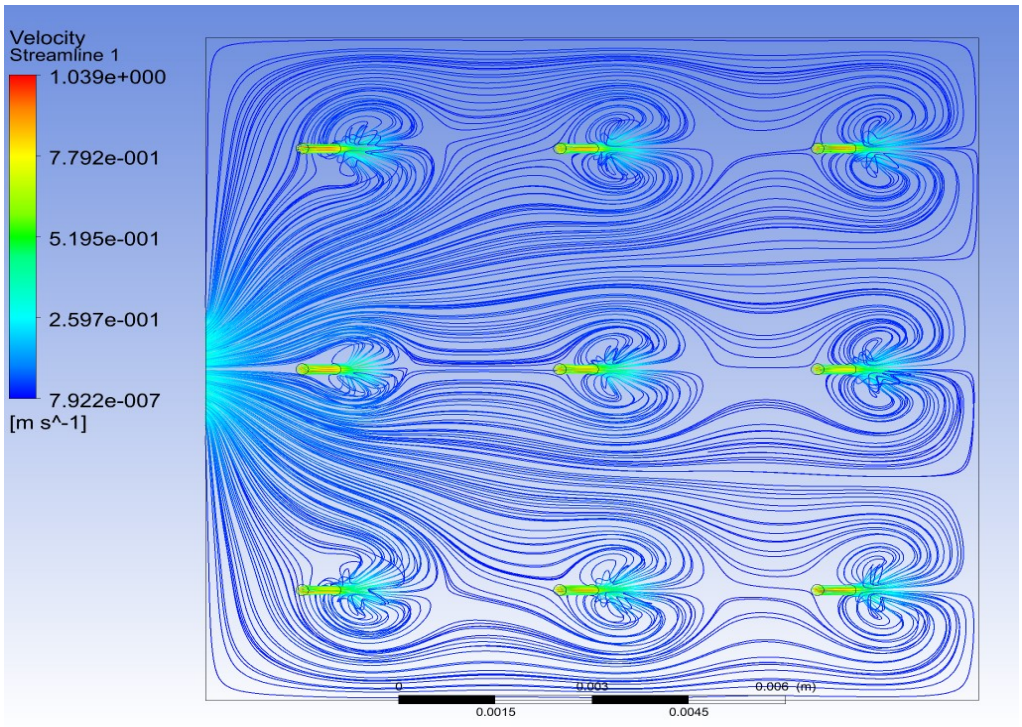

Figure 5.18: Velocity contour at solid-fluid interface across channel for 9 jet at α = 1.5.

- In figure 5.13 the average surface Temperature of fluid-solid interface is 370.2 K.
- In figure 5.14 the average surface Temperature of fluid-solid interface is 382.6 K.
- In figure 5.15 the average surface Temperature of fluid-solid interface is 397 K.
- In fig 5.15 Maximum wall temperature is at the bottom wall of the heat sink and is found to be 411.4 K and further the wall temperature increases with increase in nozzle diameter.

Table 5.3: Simulation results for 9 micro-jet heat sink

Design variable $\alpha = H_c / d_n$	**average surface Temperature of fluid-solid interface T_{avg} (K)**	**Bulk mean Temperature of fluid at outlet, T_{b2} (K)**	**Max pressure drop across the channel ΔP (kpa)**
α = 3	370.2	352	26.89
α = 2	382.6	347.7	5.476
α = 1.5	397	346	1.815

5.4 Results for 13 micro-jets impingement heat sink with different nozzle diameter:

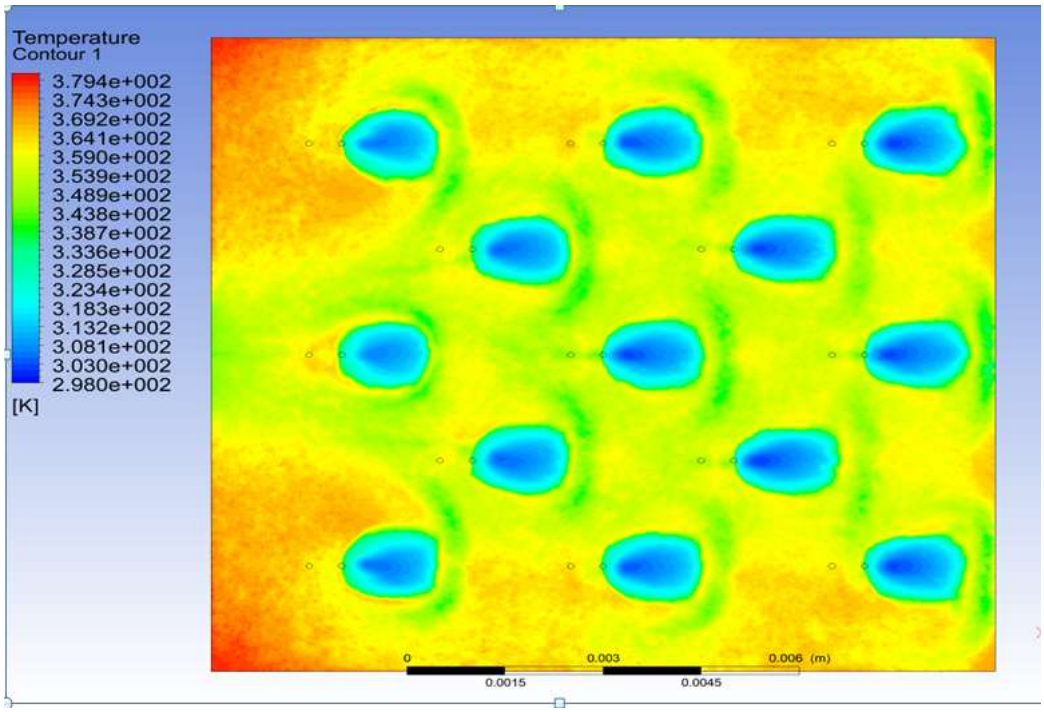

Figure 5.19: Temperature contour at solid-fluid interface across channel for 13 jet at α = 3.

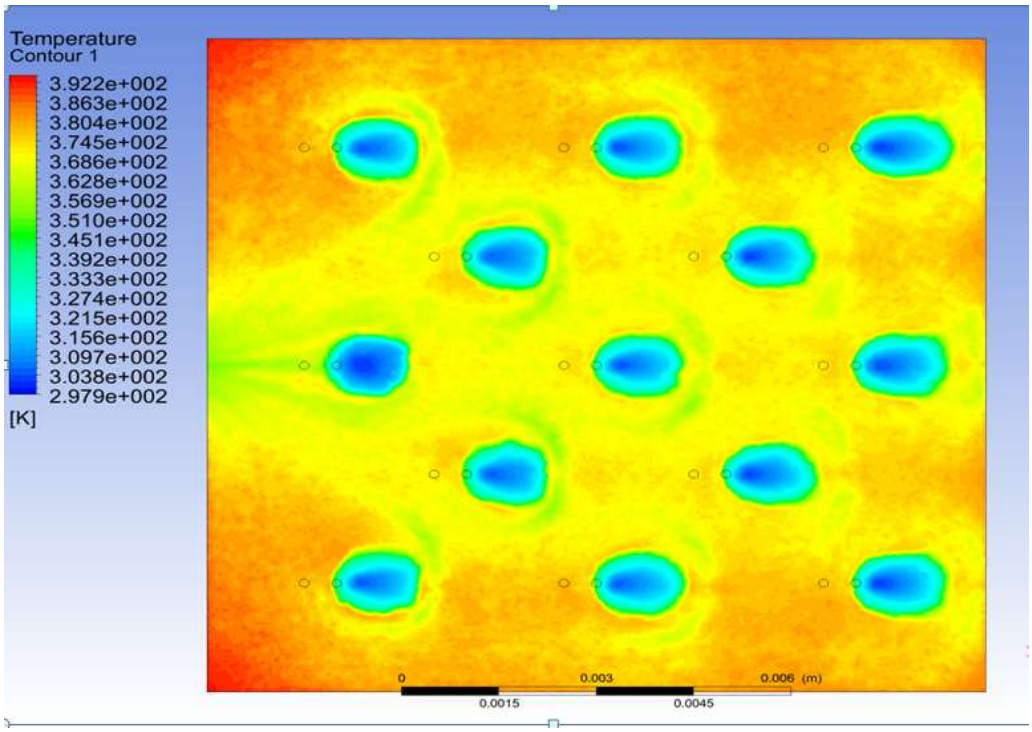

Figure 5.20: Temperature contour at solid-fluid interface across channel for 13 jet at α = 2.

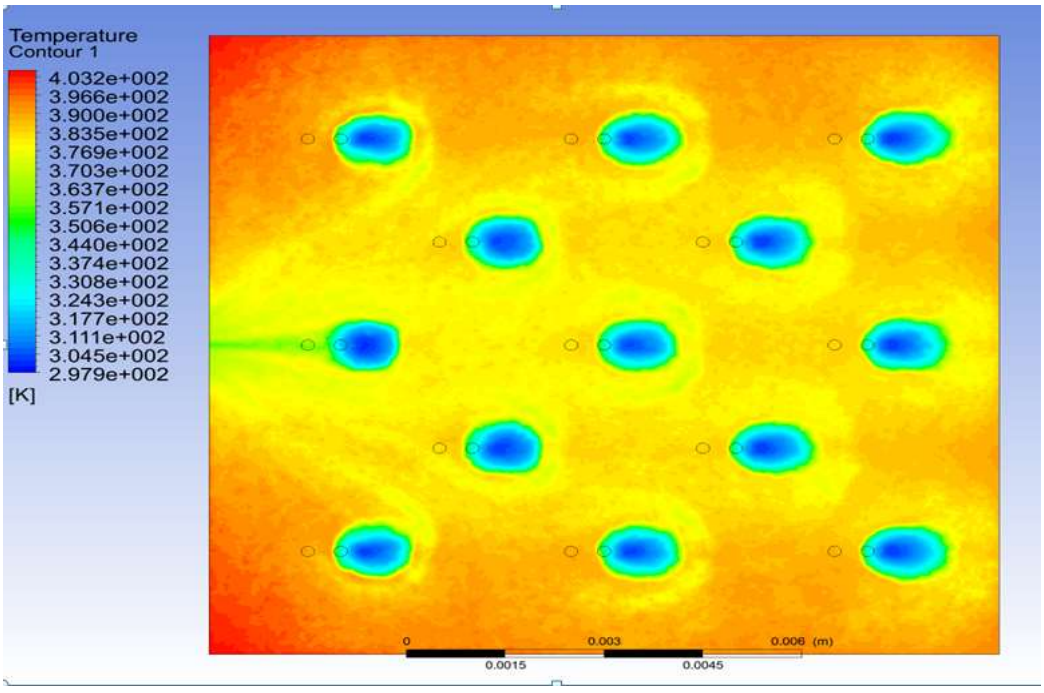

Figure 5.21: Temperature contour at solid-fluid interface across channel for 13 jet at α =1.5

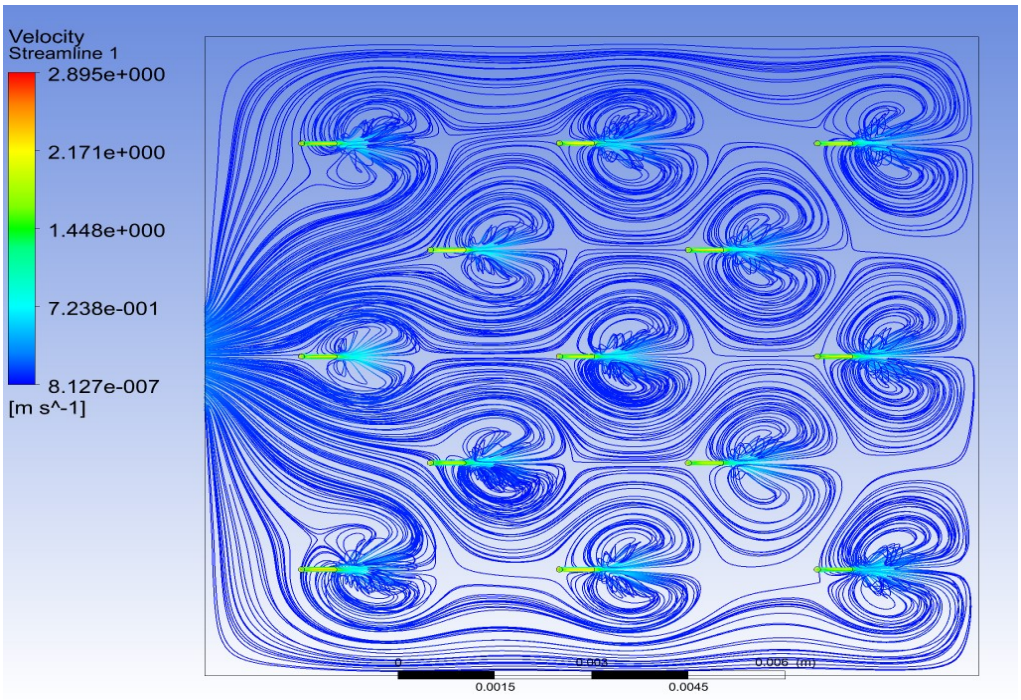

Figure 5.22: Velocity contour at solid-fluid interface across channel for 13 jet at α = 3.

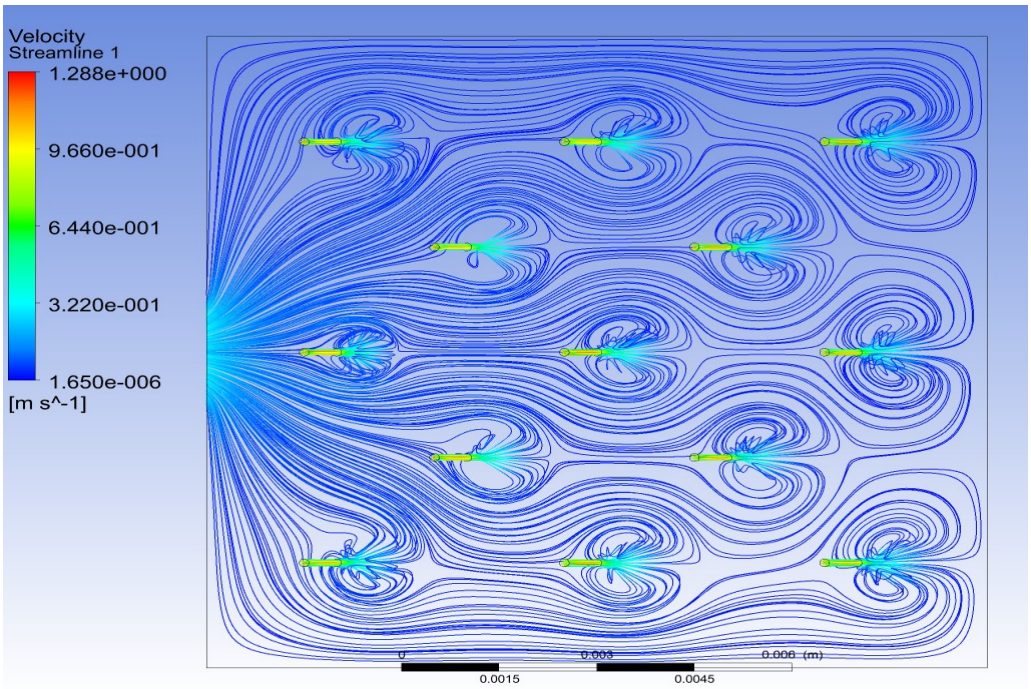

Figure 5.23: Velocity contour at solid-fluid interface across channel for 13 jet at α = 2.

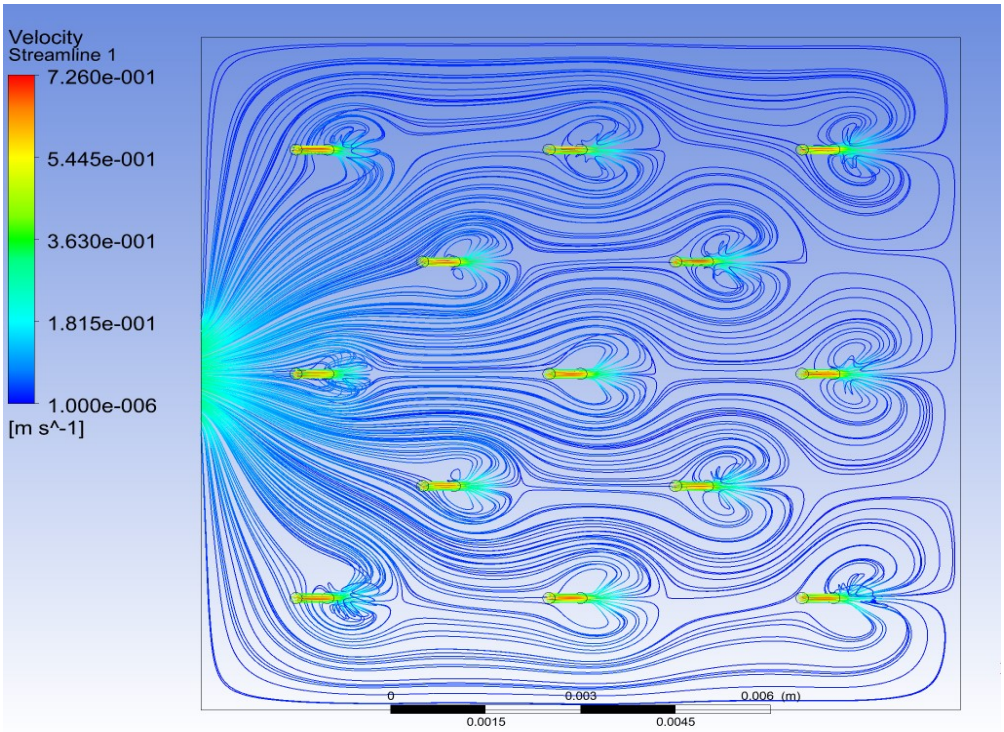

Figure 5.24: Velocity contour at solid-fluid interface across channel for 13 jet at α = 1.5.

- In figure 5.19 the average surface Temperature of fluid-solid interface is 369 K.
- In figure 5.20 the average surface Temperature of fluid-solid interface is 380.4 K.
- In figure 5.21 the average surface Temperature of fluid-solid interface is 389.6 K.
- In fig 5.21 Maximum wall temperature is at the bottom wall of the heat sink and is found to be 403.2 K and further the wall temperature increases with increase in nozzle diameter.

Table 5.4: Simulation results for 13 micro-jet heat sink

Design variable $\alpha = H_c / d_n$	**average surface Temperature of fluid-solid interface T_{avg} (K)**	**Bulk mean Temperature of fluid at outlet, T_{b2} (K)**	**Max pressure drop across the channel ΔP (kpa)**
α = 3	369	353.5	15.016
α = 2	380.4	349.2	3.051
α = 1.5	389.6	347.4	1.0832

5.5 Results for 16 micro-jets impingement heat sink with different nozzle diameter:

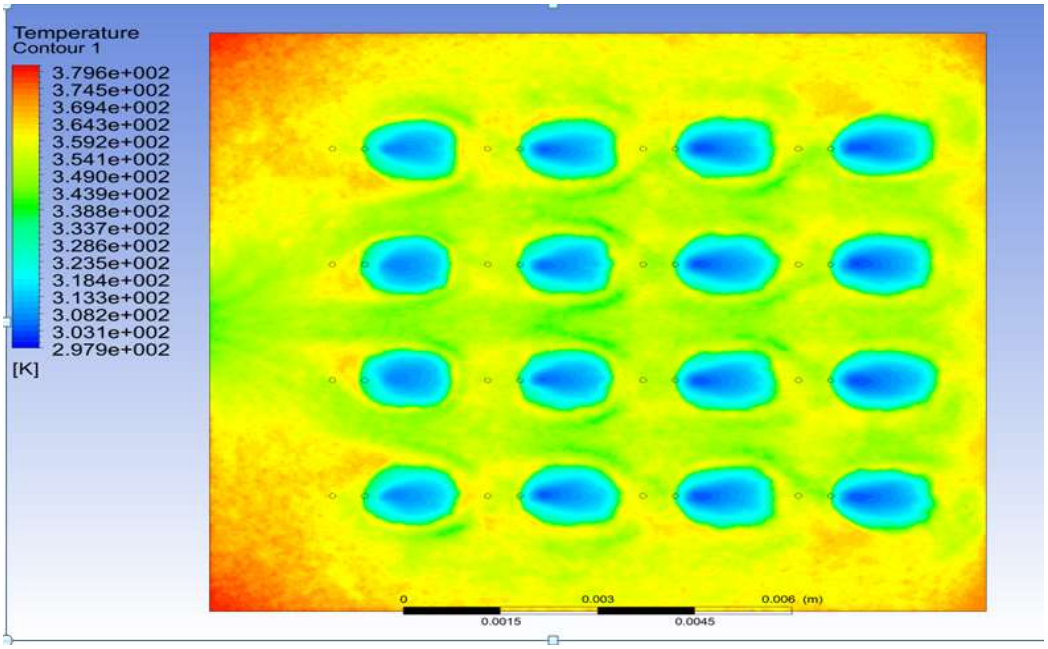

Figure 5.25: Temperature contour at solid-fluid interface across channel for 16 jet at α = 3.

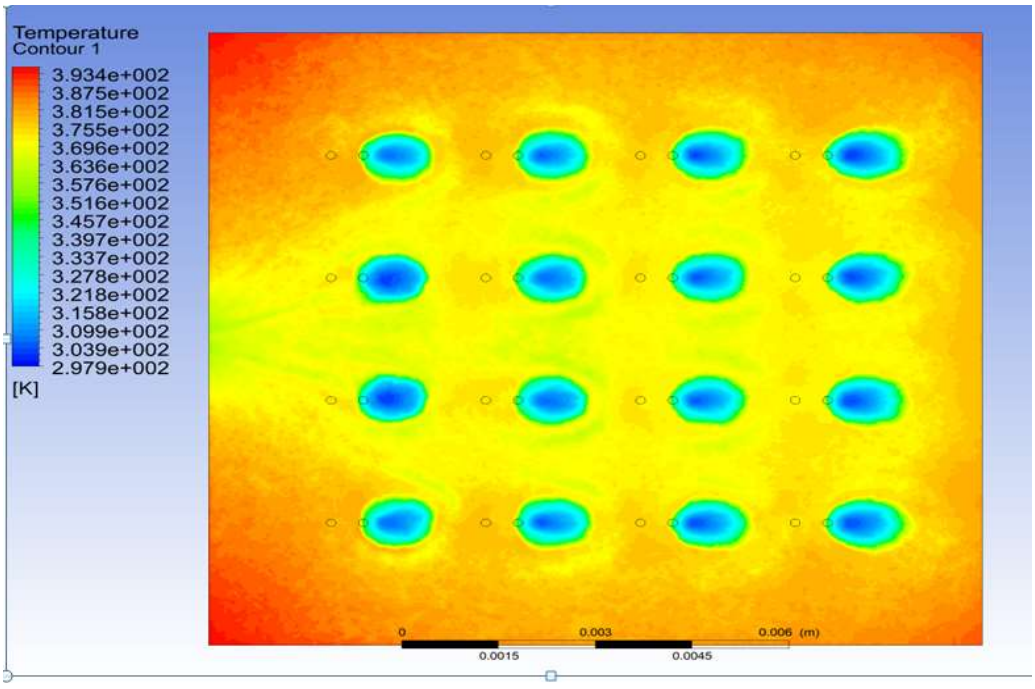

Figure 5.26: Temperature contour at solid-fluid interface across channel for 16 jet at α = 2.

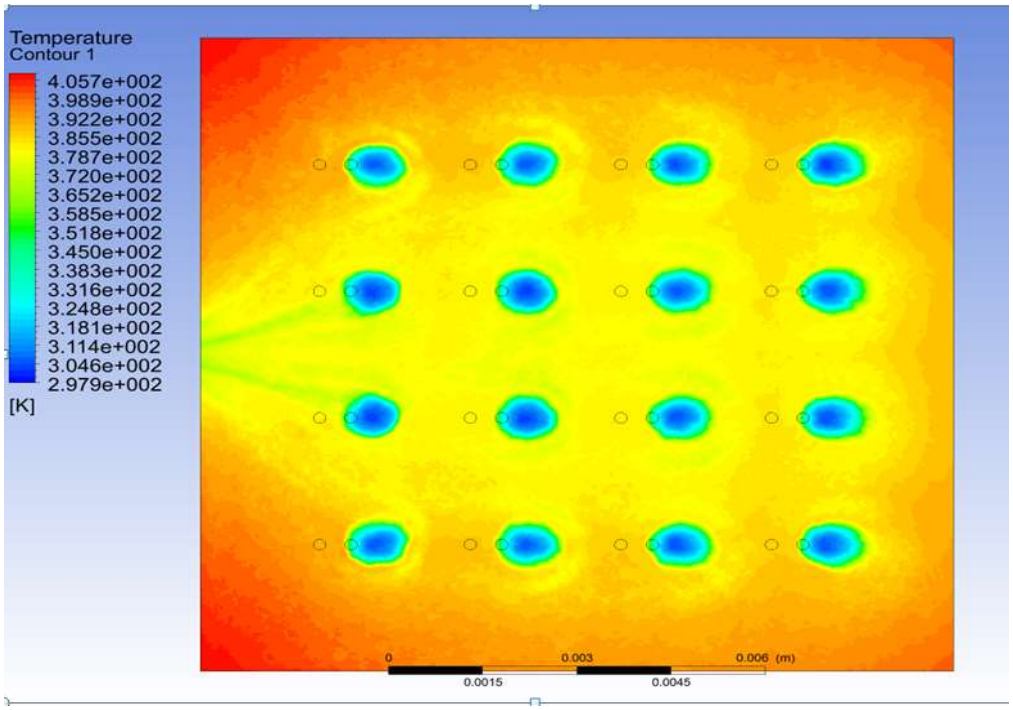

Figure 5.27: Temperature contour at solid-fluid interface across channel for 16 jet at α=1.5.

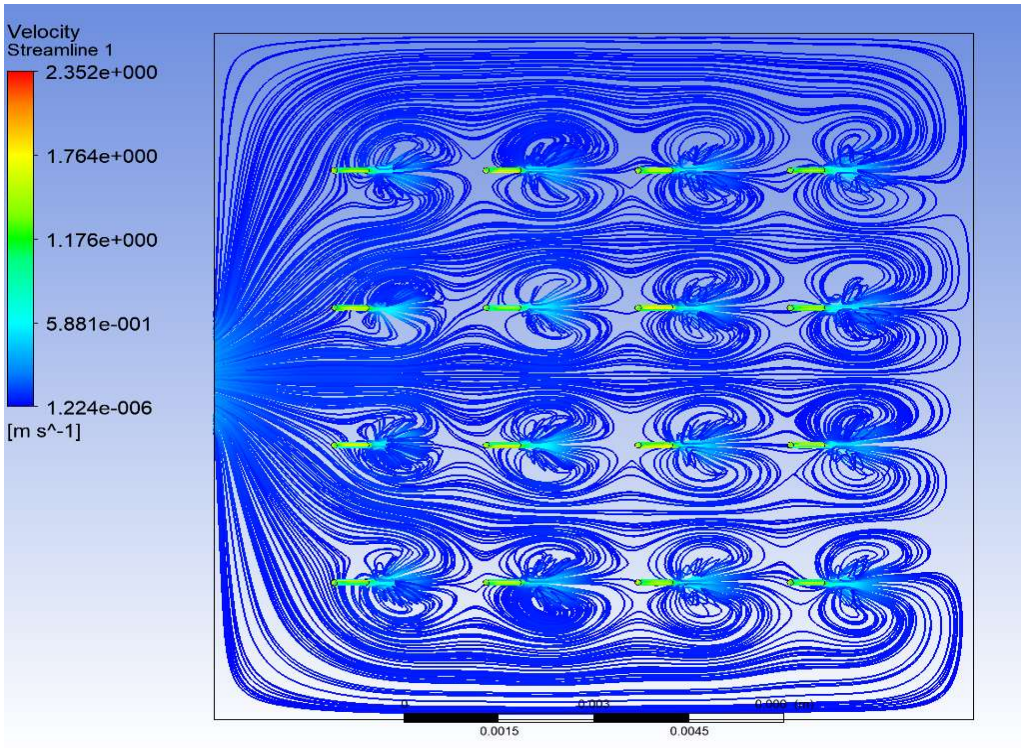

Figure 5.28: Velocity contour at solid-fluid interface across channel for 16 jet at α = 3.

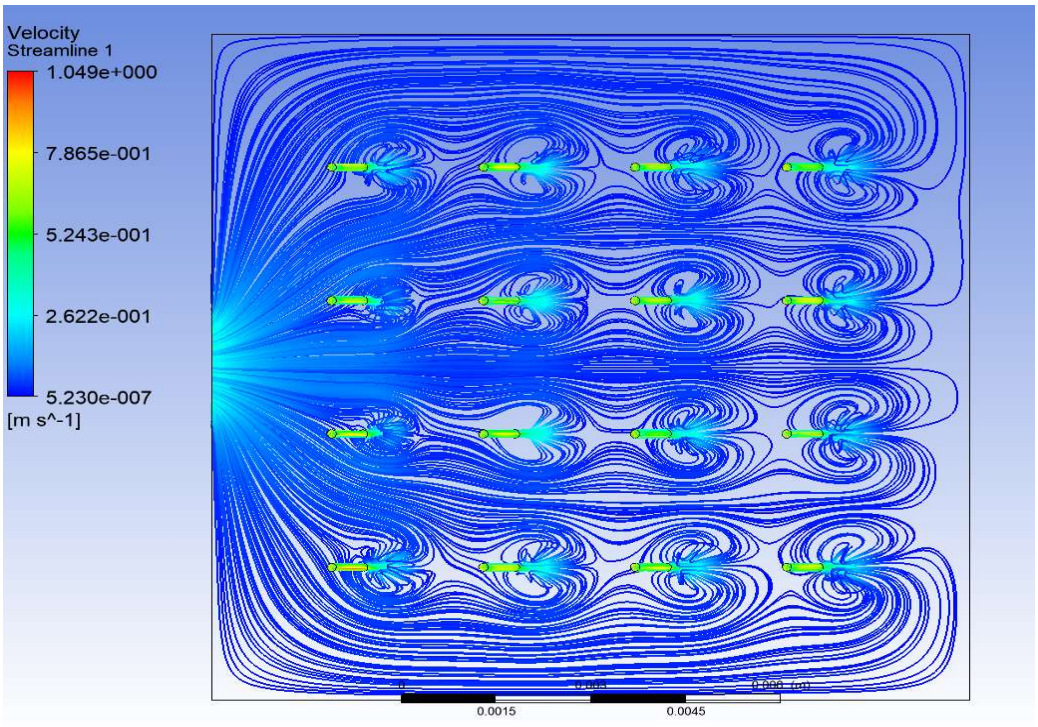

Figure 5.29: Velocity contour at solid-fluid interface across channel for 16 jet at α = 2.

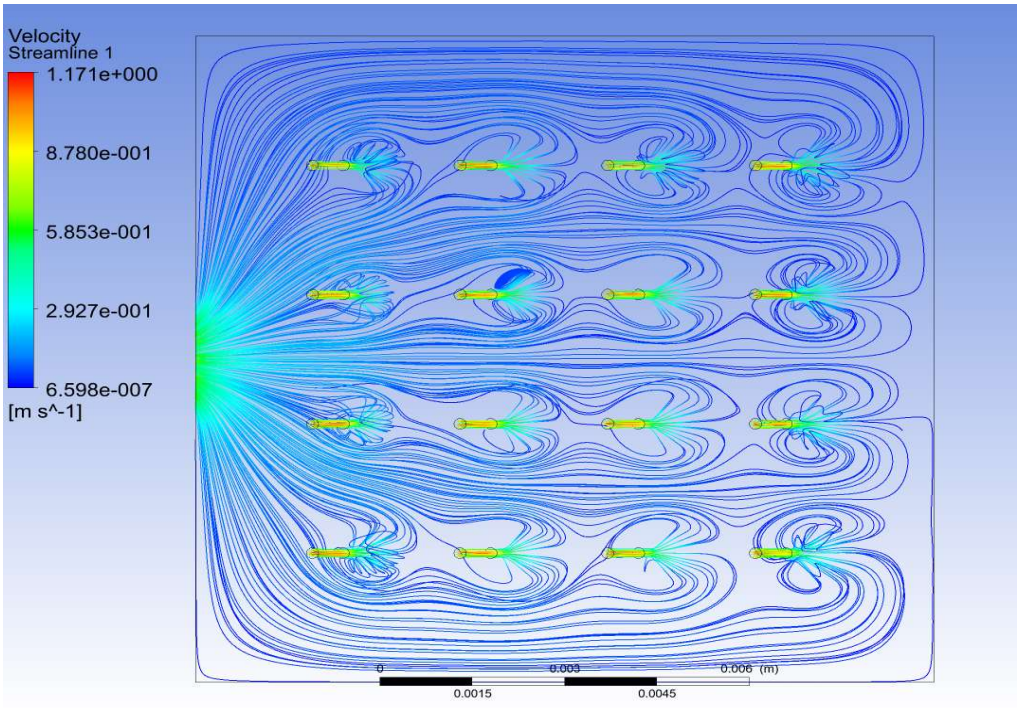

Figure 5.30: Velocity contour at solid-fluid interface across channel for 16 jet at α = 1.5.

- In figure 5.25 the average surface Temperature of fluid-solid interface is 369.4 K.
- In figure 5.26 the average surface Temperature of fluid-solid interface is 381.5 K.
- In figure 5.27 the average surface Temperature of fluid-solid interface is 392.2 K.
- In fig 5.27 Maximum wall temperature is at the bottom wall of the heat sink and is found to be 405.7 K and further the wall temperature increases with increase in nozzle diameter.

Table 5.5: Simulation results for 16 micro-jet heat sink

Design variable $\alpha = H_c / d_n$	**average surface Temperature of fluid-solid interface** T_{avg} **(K)**	**Bulk mean Temperature of fluid at outlet,** T_{b2} **(K)**	**Max pressure drop across the channel ΔP (kpa)**
α = 3	369.4	353	11.6
α = 2	381.5	349	3.0069
α = 1.5	392.2	346.9	1.0017

The above simulation results is successfully done for the different jet configurations with 3 different diameters and the result values of thermal parameters like average surface Temperature of fluid-solid interface, T_{avg} (K) , Bulk mean Temperature of fluid at outlet, T_{b2} (K) and Maximum pressure drop across the channel ΔP (kpa) are taken from the contour graphs which are evaluated in the ANSYS CFX. Further analysis is done with the help of a simple graph which shows the variation of this thermal parameters with respect to number of jets and defferent value of α.

The effect of the micro-jet design dimensions ie (α) and number of jets (n) on the thermal performance of the impingment heat sink, i.e.

a) Pressure drop across the channel ΔP (kpa).

b) Average surface Temperature of fluid-solid interface, T_{avg} (K).

c) Bulk mean Temperature of fluid at outlet, T_{b2} (K)

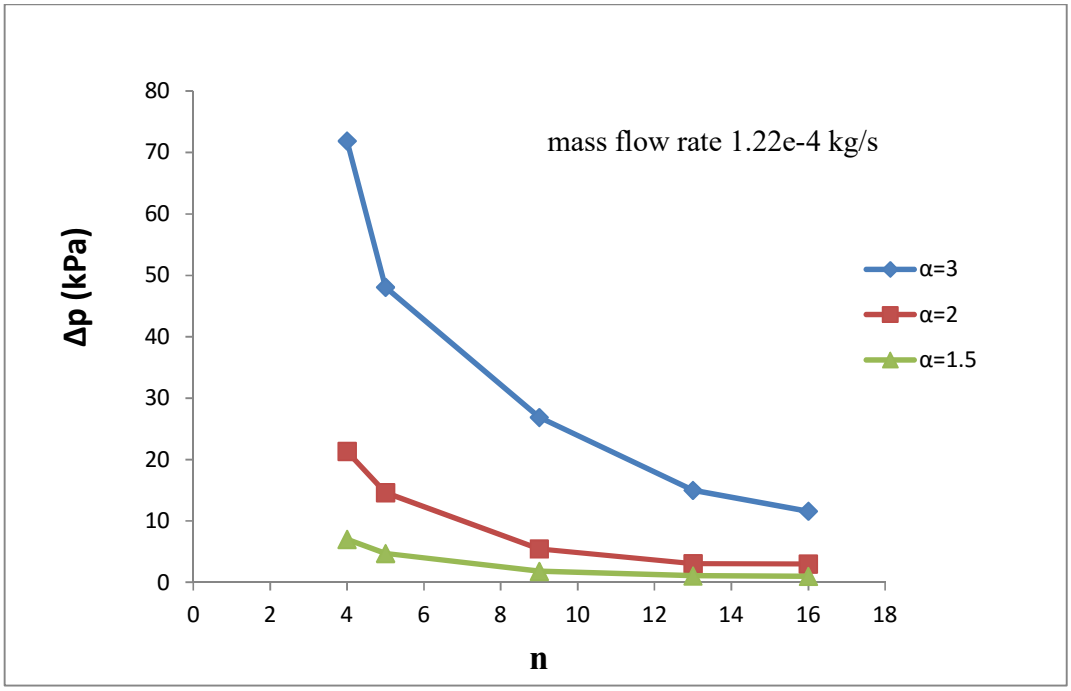

Figure 5.31: Pressure drop across the channel ΔP (kpa) v/s no. of jets (n).

The above graph shows the cumulative analysis of pressure drop across channel for 3 different diameters in which maximum pressure drop takes place for the jet diameter of 0.1mm for which design dimension α=3. As the heat transfer coefficient is the function of pressure drop along the channel so for maximum pressure drop, heat transfer coefficient is also maximum and hence greater will be the heat transfer, therefore the above result recommends minimum possible jet dimesions for designing of microchannel heat sink.

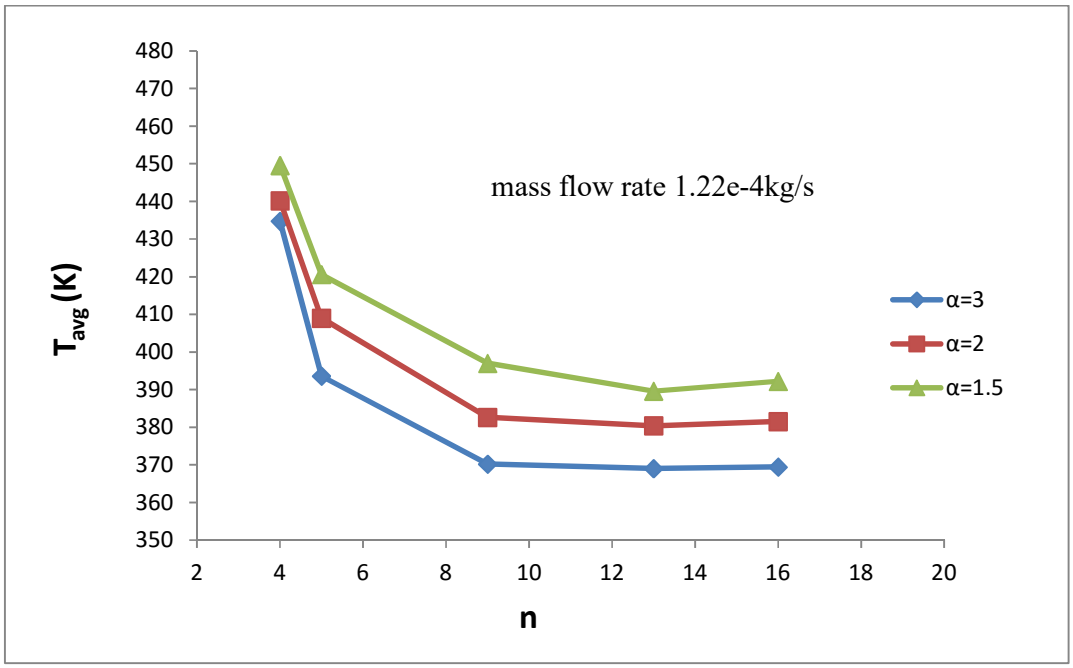

Figure 5.32: Average surface Temperature of fluid-solid interface, T_{avg} (K) v/s no. of jets (n).

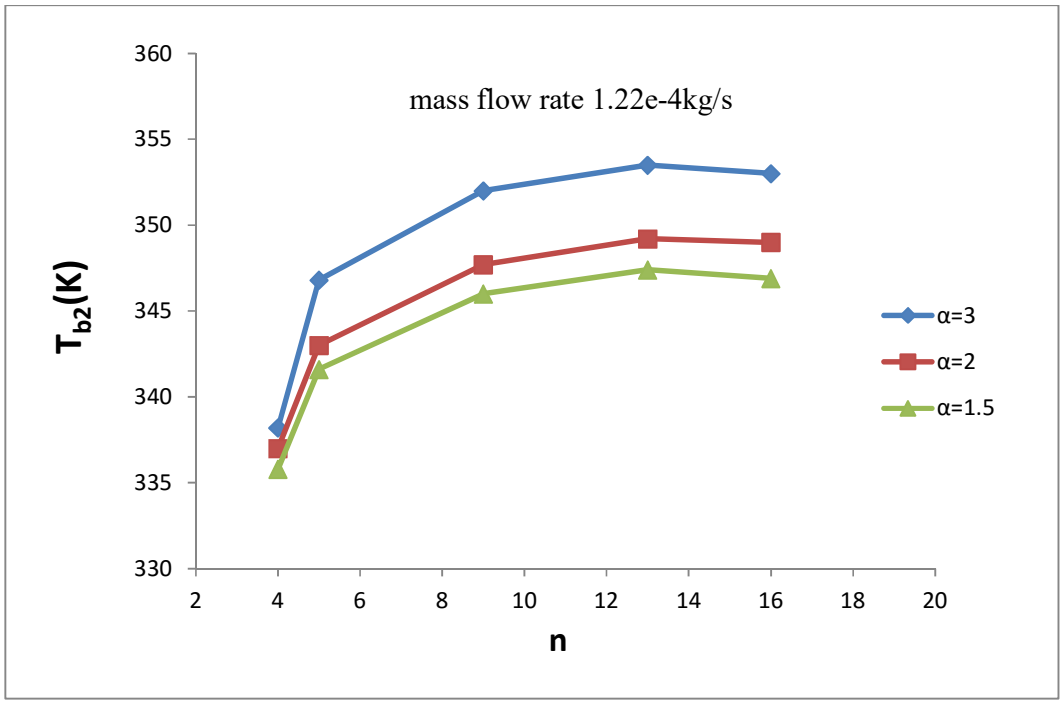

Figure 5.33: Bulk mean Temperature of fluid at outlet, T_{b2} (K) v/s no. of jets (n).

As shown in the figure 5.31, 5.32, 5.33 while increasing the number of micro-jets in general it results better uniformity in temperature distribution and pressure drop across the channel which is resulted a major reduction of average surface Temperature of fluid-solid interface, T_{avg} (K) and therefore good results in heat transfer rate with the increase in the no. of nozzles from 4 to 9. Which indicates the dominating stagnation heat transfer, and further increase in the number of nozzles from 9 to 16, it weakened stagnation heat transfer and hence the h_{avg} too.

The significant decrease in ΔP & also in average surface Temperature of fluid-solid interface, T_{avg} (K) were observed with increasing number of jets (n) until a staggered 9-jet array was reached. A further increase in the no. of micro-jets from the staggered 9-jet to 13-jet heat sink array led only to a small variations in T_{avg} (K) and ΔP as shown in fig-5.31-5.32. Now further change in the jet configuration from staggered 13-jets to an inline 16 jet-array resulting led to a slightly increase in T_{avg} (K) , even though the pressure drop decreased monotonously. While increasing number of jets the decrease in mass flow rate per jet is also obtained.

The assumed adiabatic side and upper walls of the heat sink definitely affects the uniformity of temperature distribution because near the walls high temperature are obtained. As the distance between the two micro-jets and also the distance of jets from the side-wall in inline 16 jet-array is smaller than the staggered 13-jet array, therefore later showed a maximum possible reduction in T_{avg} (K) than the former because of conjustion in fluid flow.

On the other hand, the temperature of the outgoing fluid increases with increasing number of jets. The maximum temperature drop for all three configurations, i.e. staggered 9 and 13 jet-arrays and inline 16 jet-array, was very close to each other and this results suggest that the decrease in flow rate per jet is as critical as the number of jets for the heat sink performance. The increased number of jets caused better distribution of temperaute and hence better heat transfer which consequently increased h_{avg} of the jet impingements upto certain limit.

CHAPTER-6

CONCLUSION

After all inceptions we obtained some conclusion from simulation. It has been defined in different micro-jet category of heat sink in above , a single pass constant fluid flow in multiple inclined micro-jet impingement cooling device has been modeled and solved in ANSYS CFX.

- The study examined thermal analysis i.e. pressure and temperature variation characteristics of copper-based solid substrate impingement heat sink for electronic devices cooling through CFD analysis.
- Two design variables, i.e. the ratio of channel height and nozzle diameter ($\alpha = H_c/d_n$) and the no. of jets (n) were found to affect the objective functions, i.e. the pressure drop, temperature drop and ultimately heat transfer coefficient (h) .
- Nozzle angle into impingement heat sink has been Coted the best angle suited with high temperature drop at the outlet of the system ie 45^0 angle for all micro-jets.
- The heat losses at the side and upper walls through convection and radiation are neglected for conservative analysis of the heat sink.
- Validation is done successfully for inclined 4-jet model and results were compared with the experimental results reported in [29].
- The simulation analysis of several micro dimensional jet configurations, i.e. inclined 4 jet, 5 jet, 9 jet 13-jet and 16-jet heat sink with different jet diameters, was examined to determine the temperature and pressure-drop characteristics.
- The increased number of jets caused better distribution of temperature and hence better heat transfer which consequently increased h_{avg} of the jet impingements upto certain limit. Although the drop in T_{avg} (K) values for all three configurations, i.e 9 jet, 13 jet and inline 16 jet-array, were quite similar as shown in figure 5.32.
- A model design of impingement heat sink with a inclined 13-jet module showed better performance than the others among the investigated jet configurations. Therefore for the future scope we recommend that the 13 jet module gives an effective results and it can further optimized with different flow rates and type of coolant used like nano fluid, DIUF- water and performance fluid (PF- 5060).

References

[1] Tuckerman, D.B. and Pease, R.F.W., 1981. High-performance heat sinking for VLSI. IEEE Electron device letters, 2(5), pp.126-129.

[2] Knight, R.W., Hall, D.J., Goodling, J.S. and Jaeger, R.C., 1992. Heat sink optimization with application to microchannels. IEEE Transactions on Components, Hybrids, and Manufacturing Technology, 15(5), pp.832-842.

[3] Yeh, L.T., 1995. Review of heat transfer technologies in electronic equipment. Transactions of the ASME-P-Journal of Electronic Packaging, 117(4), pp.333-339.

[4] Webb, B.W. and Ma, C.F., 1995. Single-phase liquid jet impingement heat transfer. Advances in heat transfer, 26, pp.105-217.

[5] Garimella, S.V. and Rice, R.A., 1995. Confined and submerged liquid jet impingement heat transfer. Transactions-ASME-P-Journal of Heat Transfer, 117, pp.871-877.

[6] Peng, X. F., and G. P. Peterson. "Convective heat transfer and flow friction for water flow in microchannel structures." International Journal of Heat and Mass Transfer 39, no. 12 (1996): 2599-2608.

[7] Mala, G.M., Li, D. and Dale, J.D., 1997. Heat transfer and fluid flow in microchannels. International Journal of Heat and Mass Transfer, 40(13), pp.3079-3088.

[8] Wu, S., Mai, J., Tai, Y.C. and Ho, C.M., 1999, January. Micro heat exchanger by using MEMS impinging jets. In Micro Electro Mechanical Systems, 1999. MEMS'99. Twelfth IEEE International Conference on (pp. 171-176). IEEE.

[9] Lee, D.Y. and Vafai, K., 1999. Comparative analysis of jet impingement and microchannel cooling for high heat flux applications. International Journal of Heat and Mass Transfer, 42(9), pp.1555-1568.

[10] Fedorov, A.G. and Viskanta, R., 2000. Three-dimensional conjugate heat transfer in the microchannel heat sink for electronic packaging. International Journal of Heat and Mass Transfer, 43(3), pp.399-415.

[11] Ambatipudi, K.K. and Rahman, M.M., 2000. Analysis of conjugate heat transfer in

microchannel heat sinks. Numerical Heat Transfer: Part A: Applications, 37(7), pp.711-731.

[12] Qu, W. and Mudawar, I., 2002. Analysis of three-dimensional heat transfer in micro-channel heat sinks. International Journal of heat and mass transfer, 45(19), pp.3973-3985.

[13] Qu, W. and Mudawar, I., 2002. Experimental and numerical study of pressure drop and heat transfer in a single-phase micro-channel heat sink. International Journal of Heat and Mass Transfer, 45(12), pp.2549-2565.

[14] Toh, K.C., Chen, X.Y. and Chai, J.C., 2002. Numerical computation of fluid flow and heat transfer in microchannels. International Journal of Heat and Mass Transfer, 45(26), pp.5133-5141.

[15] Garimella, S.V. and Sobhan, C.B., 2003. Transport in microchannels-a critical review. Annual review of heat transfer, 13(13) pp. 460-478

[16] Liu, D. and Garimella, S.V., 2005. Analysis and optimization of the thermal performance of microchannel heat sinks. International Journal of Numerical Methods for Heat & Fluid Flow, 15(1), pp.7-26.

[17] Liu, D. and Garimella, S.V., 2005. Analysis and optimization of the thermal performance of microchannel heat sinks. International Journal of Numerical Methods for Heat & Fluid Flow, 15(1), pp.7-26.

[18] Fabbri, M. and Dhir, V.K., 2005. Optimized heat transfer for high power electronic cooling using arrays of microjets. Journal of heat transfer, 127(7), pp.760-769.

[19] Foli, K., Okabe, T., Olhofer, M., Jin, Y. and Sendhoff, B., 2006. Optimization of micro heat exchanger: CFD, analytical approach and multi-objective evolutionary algorithms. International Journal of Heat and Mass Transfer, 49(5), pp.1090-1099.

[20] Sung, M.K. and Mudawar, I., 2006. Experimental and numerical investigation of single-phase heat transfer using a hybrid jet-impingement/micro-channel cooling scheme. International journal of heat and mass transfer, 49(3), pp.682-694.

[21] Luo, X., Chen, W., Sun, R. and Liu, S., 2008. Experimental and numerical investigation of a microjet-based cooling system for high power LEDs. Heat Transfer Engineering, 29(9), pp.774-781.

[22] Husain, A. and Kim, K.Y., 2008. Shape optimization of micro-channel heat sink for micro-electronic cooling. IEEE Transactions on Components and

PackagingTechnologies, 31(2), pp.322-330.

[23] Samad, A., Lee, K.D. and Kim, K.Y., 2008. Multi-objective optimization of a dimpled channel for heat transfer augmentation. Heat and Mass Transfer, 45(2), pp.207.

[24] Michna, G.J., Browne, E.A., Peles, Y. and Jensen, M.K., 2009. Single-phase microscale jet stagnation point heat transfer. Journal of Heat Transfer, 131(11), pp.111-402.

[25] Husain, A. and Kim, K.Y., 2010. Enhanced multi-objective optimization of a microchannel heat sink through evolutionary algorithm coupled with multiple surrogate models. Applied Thermal Engineering, 30(13), pp.1683-1691.

[26] De Paz, M.L. and Jubran, B.A., 2011. Numerical modeling of multi micro jet impingement cooling of a three dimensional turbine vane. Heat and mass transfer, 47(12), pp.1561-1579.

[27] Heo, M.W., Lee, K.D. and Kim, K.Y., 2011. Optimization of an inclined elliptic impinging jet with cross flow for enhancing heat transfer. Heat and Mass Transfer, 47(6), pp.731-742.

[28] Husain, A. and Kim, K.Y., 2011. Thermal transport and performance analysis of pressure-and electroosmotically-driven liquid flow microchannel heat sink with wavy wall. Heat and Mass Transfer, 47(1), pp.93-105.

[29] Husain, A., Kim, S.M. and Kim, K.Y., 2013. Performance analysis and design optimization of micro-jet impingement heat sink. Heat and Mass Transfer, 49(11), pp.1613-1624.